SPECTRAL METHODS IN THE IDENTIFICATION OF TIME SERIES

A. Lewandowski

October 1983
WP-83-97

INTERNATIONAL INSTITUTE FOR APPLIED SYSTEMS ANALYSIS
2361 Laxenburg, Austria

FOREWORD

The analysis of time series is a very important element in much of the systems work carried out at IIASA and elsewhere. The basic principles of time series analysis were laid down by Box and Jenkins in 1970 in an approach which divided model building into three stages: model identification, parameter estimation and model validation. However, while there are many formal approaches to parameter estimation and several formal methods for model validation, the only available tool for model identification is currently visual inspection of the time series plot and autocorrelation function. This is evidently the weakest point of the Box–Jenkins methodology.

In an attempt to remedy this, Andrzej Lewandowski proposes here a new approach to Box–Jenkins model identification. In contrast to the existing tools, this approach is based on spectral methods and involves frequency analysis of ARMA models. It differs from the standard spectral approach presented in textbooks on time series analysis, although it is based on a principle well known in control engineering and circuit theory. This method provides a means of analyzing time series in some depth using only a pencil, a piece of paper, and a pocket calculator.

ANDRZEJ WIERZBICKI
Chairman
System and Decision Sciences

CONTENTS

SPECTRAL METHODS IN THE IDENTIFICATION OF TIME SERIES

A. Lewandowski

1. INTRODUCTION

Over 10 years have now passed since the publication of a book by Box and Jenkins (Box and Jenkins, 1970) describing the basic principles of time series analysis. During this period, the methodology developed by these authors has been applied to hundreds of practical problems with great success; new tools have been developed and many theoretical investigations have been performed. However, it should be pointed out that Box and Jenkins were not the first scientists working in this field — time series analysis actually began much earlier in this century (for a bibliography see Anderson, 1971). The most important feature of the Box–Jenkins approach (and, in the author's opinion, the main reason for its popularity) is the general *methodology of model building*. Box and Jenkins divided *the process of model building* into three steps:

1. *Model identification*, during which preliminary analysis is performed and an initial version (structure) of the model is determined.
2. *Parameter estimation*, during which exact values of model parameters are computed.
3. *Model validation*, during which the quality of the resulting model is examined.

According to Box and Jenkins, modeling is a process which is repeated until the model attains the desired form and accuracy. It is difficult to make any formal evaluation of the importance of each of the above stages in this process; however, it is generally accepted that the second stage is the most important and interesting of the three. The reason for this is obvious: parameter estimation provides excellent opportunities for new mathematical work, for developing computer programs and for publishing papers. The other two stages (especially model identification) are somewhat more diffuse in nature. While there are a limited number of formal approaches that can be used for model validation, model identification is almost entirely unformalized. The only available tool for model identification is "visual inspection" of the time series plot and autocorrelation function. This is evidently the weakest point of the Box–Jenkins methodology.

In the author's opinion, the role of the model identification process is frequently underestimated. Model identification is not simply a procedure for determining the structure of a model; it is a scientific process which leads to a deeper understanding of the phenomena being investigated. In many practical cases this increased knowledge of the system is more important than the resulting model. For these reasons, the author proposes a new approach for Box–Jenkins model identification. In contrast to the existing methods, this approach is based on *spectral methods* and involves *frequency analysis* of

ARMA models. However, it differs from the standard spectral approach presented in textbooks on time series analysis. The principle behind this method is well-known in control engineering and circuit theory, and has been applied successfully in these fields. The author has simply adopted this methodology for use in time series identification; it is nothing more than a way of understanding and interpreting the spectrum and hence the model itself. In the author's (admittedly subjective) opinion, spectral methods are in general more useful than time-domain methods. Spectral responses are easier to interpret, analyze and understand than time-domain responses. Moreover, spectral responses can immediately tell the experienced analyst almost everything there is to know about system dynamics — this is not the case with time-domain analysis.

It is rather difficult to explain why spectral methods play such a marginal role in time series analysis. According to Makridakis (1976):

> "...engineers, on the other hand, insist that the spectrum is a more natural quantity to compute because it expresses a time series in terms of its frequency response, which must be known for design purposes. They say that statisticians play down the value of spectral analysis mainly because they cannot think in frequency terms. Whatever the truth, the fact is that spectral analysis has found little use in the social sciences in general, mainly because it is troublesome to calculate and interpret..."

There is really only one work which extensively uses the spectral approach for model building and analysis — this is the book by Nerlowe, Grander and Carvalho (Nerlowe et al., 1979).

2. LINEARIZED TRANSFER FUNCTIONS OF ARMA MODELS

We will use here some basic concepts from z transform theory (see Koopmans, 1974 or Nerlowe et al., 1979). Let

$$\{x_t\}, \quad t \in (-\infty, +\infty) \tag{1}$$

be a real sequence. The z transform of this sequence is the complex function

$$X(z) = \sum_{i=-\infty}^{+\infty} x_i z^i \tag{2}$$

and this is denoted by

$$X(z) \simeq x_t \ . \tag{3}$$

Under certain conditions this transformation is invertible, and $X(z)$ uniquely characterizes the x_t (see, e.g., Cadzow, 1973).

Let us consider two time series $\{x_t\}$ and $\{u_t\}$ connected by the linear relationship (operator) G:

$$\{x_t\} = G(\{u_t\}). \tag{4}$$

By *transfer function* we mean the complex function

$$G(z) = \frac{X(z)}{U(z)} \ . \tag{5}$$

It is easy to calculate the transfer function for ARMA-type models. Taking (2) and multiplying both sides by z we obtain

$$zX(z) = \sum_{i=-\infty}^{+\infty} x_i z^{i+1} = \sum_{i=-\infty}^{+\infty} x_{i-1} z^i \ . \tag{6}$$

Thus, if

$$X(z) \simeq x_t \tag{7}$$

then

$$zX(z) \simeq x_{t-1} \ . \tag{8}$$

It follows from the above that the complex variable z can be *formally* interpreted as the shift operator B used by Box and Jenkins; in order to obtain the transfer function for this model it is sufficient to replace operator B by complex variable z. We should emphasise that this operation is *formal* — the rational functions involving B and z have the same form, but must be interpreted differently.

We shall use the term *spectral* or *frequency transfer function* to describe the following formula:

$$G(j\omega) = \frac{P(e^{-j\omega})}{Q(e^{-j\omega})} \tag{9}$$

where P and Q are respectively the numerator and denominator of the operator transfer function (from now on we will consider only rational operator transfer functions). The spectrum of the output signal $\{x_t\}$ (which is actually the time series being analyzed) is proportional to the modulus of the transfer function

$$f(\omega) \simeq |G(j\omega)| \ . \tag{10}$$

Formula (10) shows where most of the basic difficulties in interpreting spectra arise — although the structure of the transfer function itself is rather simple, the spectrum is a highly nonlinear function of frequency. It is important to note that the spectrum is the modulus of the transfer function evaluated on the unit circle.

This leads to an important question — *does the modulus of the complex function evaluated on the unit circle characterize this function uniquely*? The answer is generally *no*. If we have a function $G(z)$ such that its modulus evaluated on the unit circle is

$$f(\omega) = |G(e^{-j\omega})|$$

then the function

$$G_1(z) = G(z)\left[\frac{z-\alpha}{\frac{1}{z}-\alpha}\right]$$

will have the same modulus. But if the function $G(z)$ has the *minimum phase property* (i.e., has no poles or zeros inside the unit disc), the modulus evaluated on the unit circle will characterize the function uniquely. This is one of the most important problems in the theory of signal processing, electrical circuit theory and automatic control. Some discussion of this issue can be found in Robinson (1981).

We could also ask ourselves another question — is it possible to evaluate the modulus of $G(z)$ on another line to produce a simpler $f(\omega)$?

The real and imaginary axes appear especially attractive for this purpose. In this case a similar result can be obtained — if $G(z)$ has the minimum phase property, (i.e., it has no zeros or poles in the right half-plane), it is sufficient to know the modulus of $G(z)$ evaluated for $z = j\omega$ to determine this function uniquely. Moreover, $|G(j\omega)|$ has a much simpler structure than $|G(e^{-j\omega})|$ (it contains no trigonometric functions). However, this is of little immediate use to us since it is unreasonable to expect that the transfer function of the time series under study will have no poles or zeros in the right half-plane. But there is a very simple way to avoid this difficulty — to transform the region outside the unit circle into the left half-plane and to evaluate the modulus of the resulting function on the imaginary axis. Let us consider the transformation

$$\lambda = \frac{1-z}{1+z} . \tag{11}$$

This transformation has the following properties:

1. It is invertible, i.e.,

$$z = \frac{1-\lambda}{1+\lambda} \quad . \tag{12}$$

2. It transforms the region outside the unit circle in the complex plane z into the left half of the complex plane λ; the unit circle is transformed into the imaginary axis (see Silverman, 1975).

3. If we apply this transformation to the rational transfer function then the resulting function will also be rational; if the ARMA model is stable and invertible, all of the poles and zeros of the resulting rational function will be in the left half of the λ complex plane. This means that the resulting transfer function has the *minimum phase property* (Robinson, 1981).

The minimum phase property is very important here — as pointed out above, it allows us to work with the modulus of the function rather than with the function itself. The rational function

$$g(\lambda) = \frac{P\left[\frac{1-\lambda}{1+\lambda}\right]}{Q\left[\frac{1-\lambda}{1+\lambda}\right]} = \frac{p(\lambda)}{q(\lambda)} \tag{13}$$

will be called the *linearized transfer function* ; analogously,

$$g(j\omega) = \frac{p(j\omega)}{q(j\omega)} \tag{14}$$

will be called the *linearized frequency transfer function*, and

$$\tilde{f}(\omega) = |g(j\omega)| \tag{15}$$

the *linearized spectral density function* (LSDF). We now have to investigate the relationship between the standard spectrum and the linearized spectrum.

Note that, instead of calculating the spectrum by making the substitution

$$z = e^{-j\omega} \quad , \tag{16}$$

we can use

$$z = \frac{1-j\omega}{1+j\omega} , \tag{17}$$

which is the Pade approximation (or linearization) of exponential function (16). This is the source of the name *"linearized spectrum"*. It is not difficult to find the exponential form of (17):

$$\frac{1-j\omega}{1+j\omega} = e^{-2j \arctan \omega} . \tag{18}$$

Comparing this result with (16), we conclude immediately that the linearized spectrum can be interpreted as *a standard spectrum with a distorted frequency scale*. It follows from this that we do not need special tools to calculate the linearized spectrum — it is necessary only to have a special chart with a suitably chosen frequency axis. Note also that, in contrast to the standard frequency transfer function, (14) is a rational function of frequency; this is the basic reason why the approach simplifies spectral analysis. (It should be pointed out that this transformation has also been used in control engineering for the design and analysis of sampled data control systems, see, e.g., Bishop, 1975).

3. ASYMPTOTIC FREQUENCY RESPONSES OF ARMA MODELS

We will now consider how to plot the linearized spectrum of a given transfer function. It will be shown that this is relatively easy, even for high-order models with a complex structure. This is not the case for autocorrelation function (ACFs) — in order to calculate the theoretical ACF it is generally necessary to use a computer. Only in very simple cases is it possible to calculate this function analytically. In the author's opinion, the basic advantage of the method lies in this property of the linearized spectrum, which makes it

possible to *understand and interpret* spectra for even the most complex models. We shall demonstrate the use of the linearized spectrum by analyzing the basic components of an ARMA model.

3.1. Linearized Spectrum of an MA Model

In this section we will consider the moving average MA(1) model

$$G(z) = 1 - \vartheta z \quad . \tag{19}$$

After applying the transformation (11) we obtain

$$g(\lambda) = 1 - \vartheta\left\{\frac{1-\lambda}{1+\lambda}\right\} = \frac{(1-\vartheta)\left\{1+\frac{1+\vartheta}{1-\vartheta}\lambda\right\}}{1+\lambda} \tag{20}$$

and, analogously,

$$g(j\omega) = K\left\{\frac{1+j\vartheta'\omega}{1+j\omega}\right\} \tag{21}$$

where

$$K = 1 - \vartheta \quad , \tag{22}$$

$$\vartheta' = \frac{1+\vartheta}{1-\vartheta} \quad . \tag{23}$$

Let us consider the logarithm of the modulus of (21). The frequency transfer function (21) can be expressed as the ratio of two polynomials:

$$p(j\omega) = 1 + j\vartheta'\omega \quad , \tag{24}$$

$$q(j\omega) = 1 + j\omega \quad . \tag{25}$$

The logarithm of the modulus of (24) has the form

$$\log|p(j\omega)| = \frac{1}{2}\log(1 + \vartheta'^2\omega^2) \quad . \tag{26}$$

For very low frequencies ω, i.e., when

$$\vartheta'\omega \ll 1 \ , \tag{27}$$

we have

$$\log|p(j\omega)| \simeq 0 \ . \tag{28}$$

In the opposite situation, i.e., for very high frequencies, we have

$$\log|p(j\omega)| \simeq \log\vartheta' + \log\omega \ . \tag{29}$$

This function is equal to zero for

$$\tilde{\omega} = \frac{1}{\vartheta'} \ . \tag{30}$$

It follows from (28)–(30) that, if we choose suitable axes, the function under consideration can be approximated using two lines (which are in fact the asymptotes) —a line of zero slope below $\tilde{\omega}$, and a line of slope +1 for $\omega > \tilde{\omega}$ (see Figure 1).

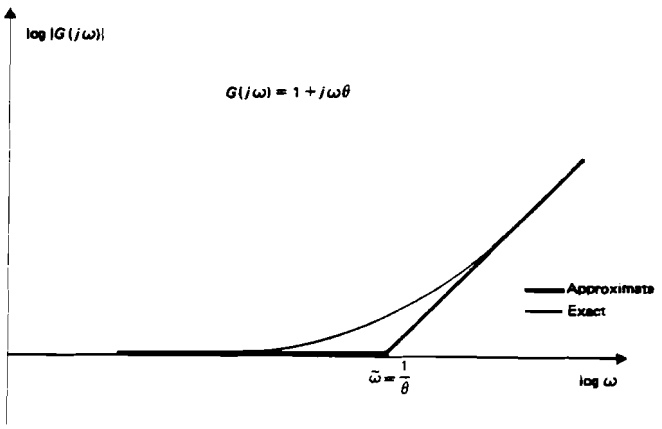

FIGURE 1 Bode plot for a transfer function with a single zero.

Figure 1 also shows that this is a reasonably good approximation of (26). This construction (the asymptotes of the frequency response function) is known as a *Bode plot*; this method of analyzing the frequency response function is one of the basic tools in electronics and control engineering (see D'Azzo and Houpis, 1975; Lago and Benningfield, 1979; Sage, 1981). It is now very easy

to construct the Bode plot for an MA(1) model. It is only necessary to bear in mind that

$$\log|g(j\omega)| = \log K + \log|p(j\omega)| - \log|q(j\omega)| \tag{31}$$

and perform a very simple graphical operation (see Figure 2). The shape of the

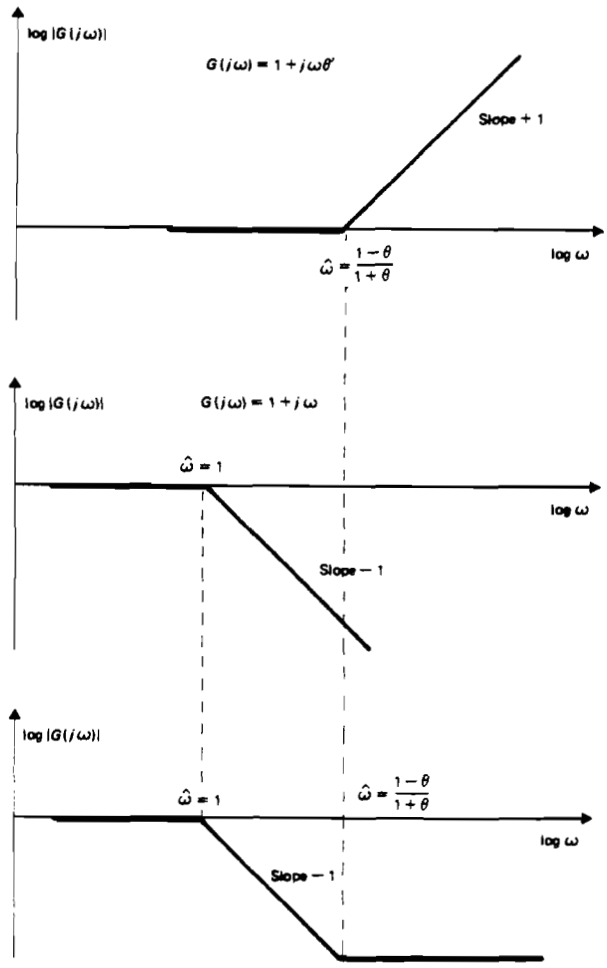

FIGURE 2 Graphical procedure for constructing the Bode plot for an MA(1) model.

Bode plot depends on the value of ϑ — one important conclusion is that the Bode plot of an MA(1) model *always has a pole at* $\omega = 1$. Possible Bode plots for an MA(1) model are presented in Figure 3. Both asymptotic plots and exact values of (21) are displayed, showing that the Bode plot represents a reasonably good approximation.

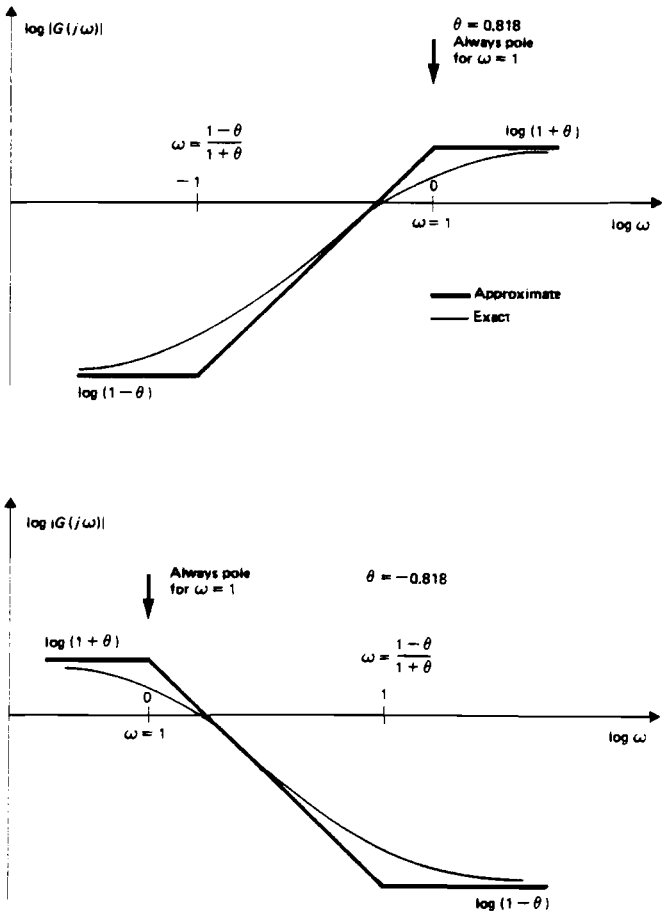

FIGURE 3 Possible Bode plots for a general moving average MA(1) model.

3.2. Linearized Spectrum of an AR(1) Model

The transfer function of an autoregressive AR(1) model has the following form:

$$G(z) = \frac{1}{1-\vartheta z} \,. \tag{32}$$

After transformation we obtain

$$g(\lambda) = \frac{1}{1-\vartheta\dfrac{1-\lambda}{1+\lambda}} = \frac{1+\lambda}{(1-\vartheta)\left[1+\dfrac{1+\vartheta}{1-\vartheta}\lambda\right]} \tag{33}$$

and, analogously,

$$g(j\omega) = \frac{1+j\omega}{K(1+\vartheta' j\omega)} \,. \tag{34}$$

We will not repeat all the arguments from the previous section — the same methodology can be used directly to construct a Bode plot for an AR(1) model. The only difference is that the frequency response of an AR(1) model *always has a zero for* $\omega = 1$. Possible Bode plots for an AR(1) model are presented in Figure 4.

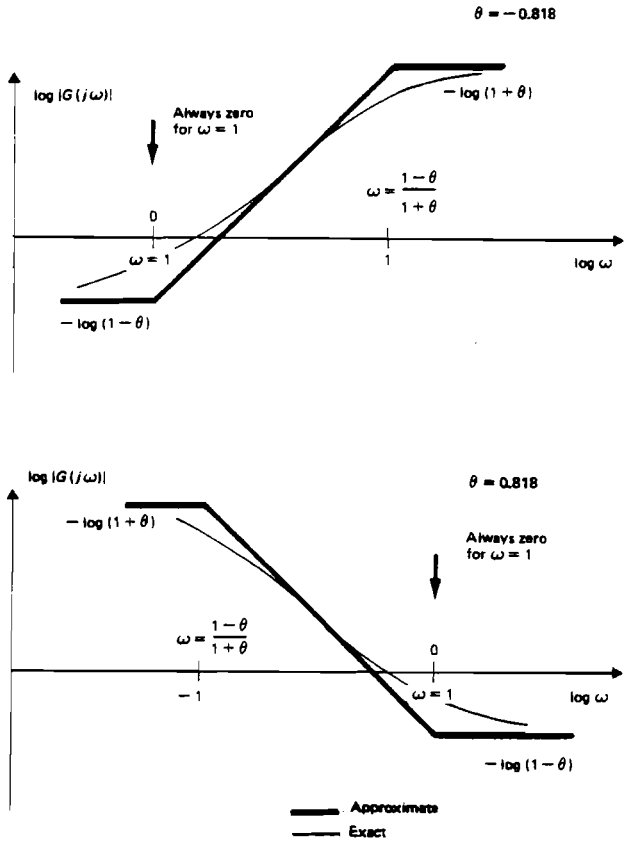

FIGURE 4 Possible Bode plots for an autoregressive AR(1) model.

3.3. Linearized Spectrum of an ARMA(1,1) Model

Using the methodology described in the previous sections, it is now very easy to construct the Bode plot for a simple autoregressive moving average ARMA(1,1) model. All we have to do is write its transfer function

$$G(z) = \frac{1-\vartheta z}{1-\varphi z} \tag{35}$$

and transformed transfer function

$$g(\lambda) = \frac{(1-\vartheta)\left[1+\frac{1+\vartheta}{1-\vartheta}\lambda\right]}{(1-\varphi)\left[1+\frac{1+\varphi}{1-\varphi}\lambda\right]} . \tag{36}$$

This function has one pole and one zero. The corresponding Bode plot can be derived immediately — the basic steps of this procedure are presented in Figure 5.

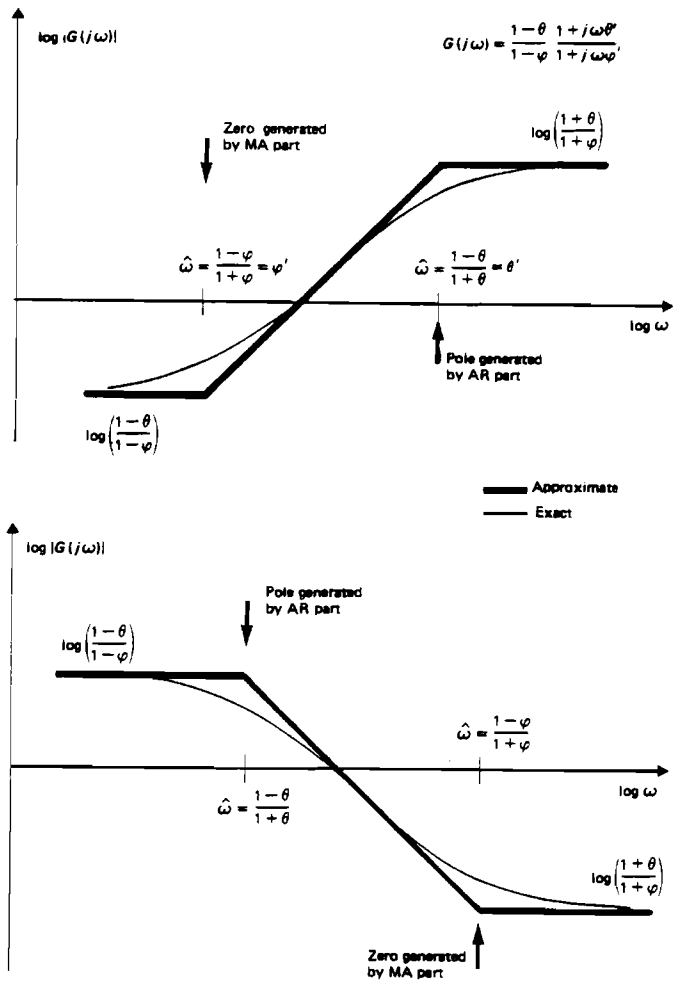

FIGURE 5 Possible Bode plots for an autoregressive moving average ARMA(1,1) model.

3.4. Linearized Spectrum of an AR(2) Model with Complex Roots

This situation is more complicated than those dealt with previously. We introduce the transfer function in a form commonly used in textbooks on time series analysis:

$$G(z) = \frac{1}{1-\vartheta_1 z - \vartheta_2 z^2} \,. \tag{37}$$

After transformation this becomes

$$g(\lambda) = \frac{1}{1-\vartheta_1\left(\frac{1-\lambda}{1+\lambda}\right) - \vartheta_2\left(\frac{1-\lambda}{1+\lambda}\right)^2} = K\frac{(1+\lambda)^2}{1+\vartheta_1'\lambda+\vartheta_2'\lambda^2} \,, \tag{38}$$

where

$$K = \frac{1}{1-\vartheta_1-\vartheta_2} \,, \tag{39}$$

$$\vartheta_1' = -\frac{2(1+\vartheta_2)}{1-\vartheta_1-\vartheta_2} \,, \tag{40}$$

$$\vartheta_2' = \frac{1+\vartheta_1-\vartheta_2}{1-\vartheta_1-\vartheta_2} \,. \tag{41}$$

For several reasons it is more convenient to use the *canonical form* of the denominator of (38):

$$q(\lambda) = 1 + \frac{\lambda\ \vartheta_1'}{\left(\frac{1}{\sqrt{\vartheta_2'}}\right)\sqrt{\vartheta_2'}} = 1 + \frac{2\xi\lambda}{\omega_r} + \frac{\lambda^2}{\omega_r^2} \,. \tag{42}$$

The value

$$\omega_r = \frac{1}{\sqrt{\vartheta_2'}} \tag{43}$$

is known as the *resonance frequency*, while the parameter

$$\xi = \frac{\vartheta_1'}{2\sqrt{\vartheta_2'}} \tag{44}$$

is the so-called *damping factor*. These two factors determine the resonance

properties of the transfer function . If $\xi > 1$ the quadratic polynomial has real roots and can be represented as the product of two first-order factors; for $0 < \xi < 1$ the roots are complex and more careful analysis is necessary. Figure 6 presents the frequency responses for different values of ξ; this figure shows that, for small values of ξ (low damping) and for frequencies close to the resonance frequency, asymptotic approximation will not be very accurate.

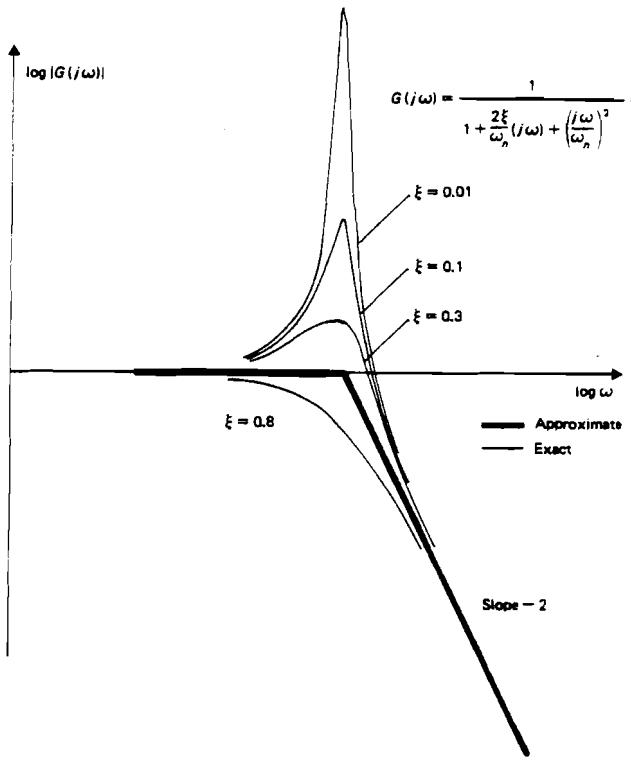

FIGURE 6 Bode plot for a second-order autoregressive model for which the transfer function has a pair of conjugate complex roots.

However, practical experience has shown that asymptotic analysis can be very useful even in this case; we shall therefore investigate the asymptotic behavior of (38). Making the substitution

$$\lambda = j\omega$$

and considering the canonical form (42), we obtain

$$g(j\omega) = K \frac{(1+j\omega)^2}{1 + \frac{2\xi j\omega}{\omega_r} - \frac{\omega^2}{\omega_r^2}} . \qquad (45)$$

The logarithm of the modulus of this function is as follows:

$$\log|g(j\omega)| = \log K + \log(1+\omega^2) - \frac{1}{2}\log\left\{\left[1-\left(\frac{\omega}{\omega_r}\right)^2\right]^2 + \frac{4\xi^2}{\omega_r^2}\right\} . \tag{46}$$

The first two terms of this formula are quite familiar and hence it is very easy to perform the asymptotic analysis. We can once again make direct use of the results obtained previously; the only difference from the MA(1) model is the slope of the asymptote of the second term, which is +2 in this case. Analysis of the third term is also straightforward — for low frequencies ω we have

$$\log\left\{\left[1-\left(\frac{\omega}{\omega_r}\right)^2\right]^2 + \frac{4\xi^2}{\omega_r^2}\right\} \simeq 0 , \tag{47}$$

while for ω sufficiently large the term $(\omega/\omega_r)^4$ is dominant and

$$\log\left\{\left[1-\left(\frac{\omega}{\omega_r}\right)^2\right]^2 + \frac{4\xi^2}{\omega_r^2}\right\} \simeq 4\log\left(\frac{\omega}{\omega_r}\right) . \tag{48}$$

Comparing this result with (46) we observe that the third term of (46) has two asymptotes — for low frequencies the slope is equal to zero, while for high frequencies it is −2. The asymptotes cross at the vertex corresponding to frequency $\omega = \omega_r$ (see Figure 6).

The following component of the frequency response (46)

$$-\frac{1}{2}\log\left\{\left[1-\left(\frac{\omega}{\omega_r}\right)^2\right]^2 + \frac{4\xi^2\omega^2}{\omega_r^2}\right\}$$

generates a peak for small ξ. The amplitude and frequency at which this peak occurs are given by (see Figure 7):

$$M = \log\left(\frac{1}{2\xi\sqrt{1-\xi^2}}\right) , \tag{49}$$

$$\omega_m = \omega_r\sqrt{1-2\xi^2} . \tag{50}$$

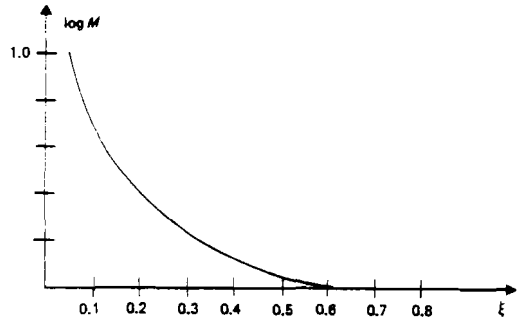

FIGURE 7 Peak height as a function of ξ in the Bode plot of the autoregressive model considered in Figure 6.

It follows from (50) that this peak exists only for sufficiently small values of the damping factor, namely for

$$\xi < 0.707 \quad . \tag{51}$$

It is now not difficult to construct the Bode plot for (45). The possible patterns are presented in Figure 8.

The only difference between the asymptotic frequency response given in Figure 8 and the frequency response of the AR(1) model is that the slope of the asymptote is equal to −2. Like the AR(1) model, an AR(2) model with complex roots *always has a double zero at* $\omega = 1$; there is also a double pole at $\omega = \omega_r$.

3.5. Linearized Spectrum of a Simple Difference Operator

One of the basic operations in Box–Jenkins methodology is the "detrending" of time series using simple differencing. Differencing is in fact a filtering process in which the transfer function of the filter has the following form:

$$G(z) = \frac{1}{1-z} \quad . \tag{52}$$

After transformation we obtain

$$g(\lambda) = \frac{1}{1-\dfrac{1-\lambda}{1+\lambda}} = \frac{1+\lambda}{2\lambda} \quad . \tag{53}$$

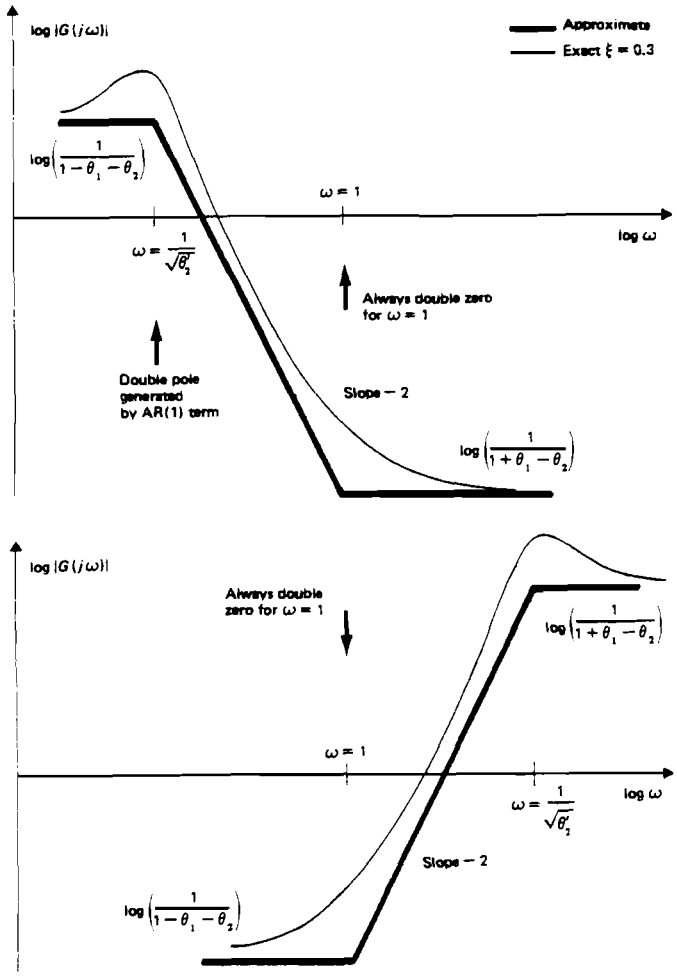

FIGURE 8 Possible Bode plots for a general autoregressive second-order model for which the transfer function has a pair of conjugate complex roots.

The resulting transfer function has *a pole at* $\omega = 0$. It is not difficult to plot the Bode diagram for this case: the asymptotic Bode plot for $1+\lambda$ has been described in previous sections, and we will not describe it again here. Consider the transfer function

$$g(\lambda) = \frac{1}{\lambda} . \tag{54}$$

Substituting $\lambda = j\omega$ and calculating the modulus, we obtain

$$\log |g(j\omega)| = -\log\omega . \tag{55}$$

It is clear from (55) that in this case the Bode plot is a line with slope -1 for every value of the frequency ω. Combining the plots for the numerator and denominator of (53), we obtain the pattern presented in Figure 9. The plot is similar to that obtained for the simple AR(1) model, except that the left vertex of the plot corresponding to the value of ϑ is shifted to minus infinity.

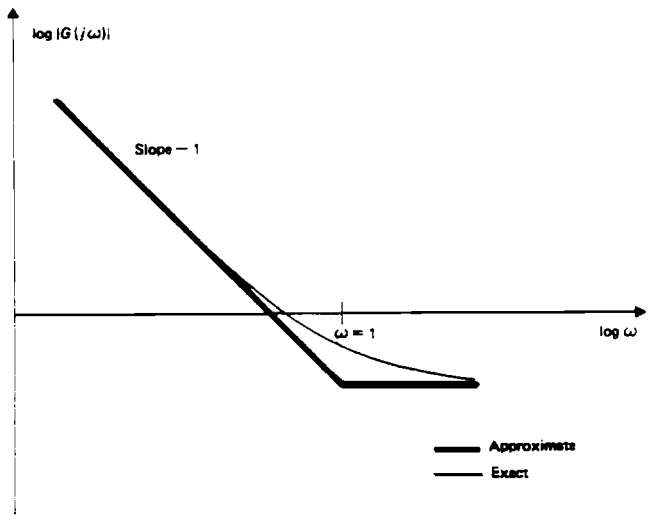

FIGURE 9 Bode plot for a simple difference operator.

3.6. Linearized Spectrum of a Seasonal Difference Operator

Another important operation in the Box–Jenkins approach is seasonal differencing. The linear filter corresponding to this operation has the following transfer function:

$$G(z) = \frac{1}{1-\vartheta z^{n}} \tag{56}$$

where n is the periodicity of the time series. After transformation we obtain

$$g(\lambda) = \frac{1}{1-\vartheta\left[\frac{1-\lambda}{1+\lambda}\right]^{n}} \tag{57}$$

and, consequently,

$$g(j\omega) = \frac{1}{1-\vartheta\left[\frac{1-j\omega}{1+j\omega}\right]^n} \quad . \tag{58}$$

Rearranging the above equation we obtain

$$g(j\omega) = \frac{(1+j\omega)^n}{(1+j\omega)^n - \vartheta(1-j\omega)^n} \quad . \tag{59}$$

We shall now analyze the denominator of the above formula. Since

$$1 + j\omega = \sqrt{1+\omega^2}e^{j\varphi} \quad , \quad \varphi = \arctan\omega \tag{60}$$

$$1 - j\omega = \sqrt{1+\omega^2}e^{-j\varphi} \quad , \quad \varphi = \arctan\omega \tag{61}$$

we deduce that

$$(1+j\omega)^n - \vartheta(1-j\omega)^n = (1+\omega^2)^{\frac{n}{2}}\left[(1-\vartheta)\cos n\varphi - j(1+\vartheta)\sin n\varphi\right] \quad . \tag{62}$$

The modulus of this function has the form

$$|(1+j\omega)^n - \vartheta(1-j\omega)^n|^2 = (1+\omega^2)^n[1+\vartheta^2-\vartheta\cos 2n\varphi] \tag{63}$$

and consequently

$$|g(j\omega)|^2 = \frac{1}{1+\vartheta^2-2\vartheta\cos 2n\varphi} \quad . \tag{64}$$

For low frequencies we have

$$|g(j\omega)|^2 \simeq \frac{1}{(1-\vartheta)^2} \quad . \tag{65}$$

For high frequencies the situation is more complicated:

$$|g(j\omega)| \simeq \begin{cases} \dfrac{1}{(1+\vartheta)^2} & \text{for } n = 1,3,5,\ldots \\ \dfrac{1}{(1-\vartheta)^2} & \text{for } n = 2,4,6,\ldots \end{cases} \tag{66}$$

It is clear that, for $\vartheta > 0$, $|g(j\omega)|$ has a maximum for those frequencies for which $\cos 2n\varphi = 1$, i.e.,

$$\hat{\omega} = \tan\left[\frac{k\pi}{n}\right] \quad \text{for } 0 < k < \frac{n}{2} . \tag{67}$$

For these frequencies the height of the peak is

$$|g(j\hat{\omega})|^2 = \frac{1}{(1-\vartheta)^2} . \tag{68}$$

Analogously, for $\vartheta > 0$, $|g(j\omega)|$ takes its minimum value for those frequencies for which $\cos 2n\varphi = -1$, i.e.,

$$\hat{\omega} = \frac{(2k+1)\pi}{2n} \quad \text{for } 0 \leq k < \frac{n-1}{2} . \tag{69}$$

For $\vartheta < 0$ the positions of the maximum and minimum are reversed, i.e., $|g(j\omega)|$ has a maximum for $\hat{\omega}$ given by (69) and a minimum for $\hat{\omega}$ given by (67). It is also important to know the position of the zeros and poles of the transfer function under investigation. There is a zero of multiplicity n at $\omega = 1$; the position of the poles can also be determined very easily. Consider the poles of (56). It is obvious that for $\vartheta > 0$ this transfer function has a real pole

$$z_1 = \vartheta^{-\frac{1}{n}} \tag{70}$$

and that for even n

$$z_2 = -z_1 \tag{71}$$

is also a pole.

Making our transformation, we conclude that the corresponding poles in the λ complex plane are as follows:

$$\lambda_1 = \frac{1-\vartheta^{-\frac{1}{n}}}{1+\vartheta^{-\frac{1}{n}}} , \tag{72}$$

and for even n

$$\lambda_2 = \frac{1+\vartheta^{-\frac{1}{n}}}{1-\vartheta^{-\frac{1}{n}}} \quad . \tag{73}$$

For $\vartheta < 0$ and odd n we still have the pole determined by (70); for even n there are no real poles. The general expression for the poles of (56) is very simple (for $\vartheta > 0$):

$$z_k = \vartheta^{-\frac{1}{n}}\left[\cos\frac{2k\pi}{n} + j\sin\frac{2k\pi}{n}\right] \qquad k = 0,1,\ldots,n-1 \quad . \tag{74}$$

After transformation, each pair of conjugate roots in the z complex plane is transformed into a pair of conjugate roots in the λ complex plane; thus, for each such pair there will be a corresponding quadratic factor in the denominator of $g(\lambda)$:

$$(\lambda-\lambda_k)(\lambda-\bar{\lambda}_k) = \lambda^2-\lambda(\lambda_k+\bar{\lambda}_k) + \lambda_k\bar{\lambda}_k \quad . \tag{75}$$

Comparing this formula with the results of our analysis for a simple AR(2) model with complex roots, we deduce immediately that the resonance frequency is

$$\omega_r^2 = \lambda_k\bar{\lambda}_k \quad . \tag{76}$$

Simple algebraic transformations lead to

$$\omega_r^2 = \frac{(1-r)^2 + (1+r)^2\omega_p^2}{(1+r)^2 + (1-r)^2\omega_p^2} \tag{77}$$

where $r = \vartheta^{-\frac{1}{n}}$ and ω_p is the frequency corresponding to a peak on the frequency response plot. It is easy to see that for $\vartheta \simeq 1$ (which is usually the case) we have

$$\omega_r \simeq \omega_p \quad . \tag{78}$$

A similar result can be obtained for $\vartheta < 0$. Now we have enough information to construct the Bode plot for the transfer function under investigation. The basic steps of the procedure are presented in Figure 10. It is important to note that the pure seasonal differencing operator (with $\vartheta = 1$) will generate infinite peaks in its frequency response, and thus cannot be interpreted using this technique.

3.7. Linearized Spectrum of a General ARMA Model

Using the results of the previous sections we can construct a Bode plot for a general ARMA model. This model can be given in terms of transfer functions as a product of the simple factors considered in the previous sections. On calculating the transformed transfer function, the frequency response and its logarithm, we conclude that the Bode plot of a general ARMA model can be obtained as the *sum of the Bode plots of its component factors*. This is true for both asymptotic and exact plots. The asymptotic plots can be constructed without any problem; it is sufficient to know where the zeros and poles of the transfer function occur. This is usually the first step of the procedure; in the next, the exact function is plotted. This is also quite straightforward, requiring only a pocket calculator (see Figure 11).

4. MODEL IDENTIFICATION USING BODE PLOTS

In this section we will investigate the inverse procedure — given the frequency response function, to find the generating transfer function $G(z)$.

This is precisely the problem of model identification; however, we shall use the spectrum instead of the autocorrelation function as in the Box–Jenkins approach. We will not consider the possible ways of calculating the spectrum here; there are many methods that could be used (see Appendix A). We shall simply assume that the spectrum can be calculated for the time series being

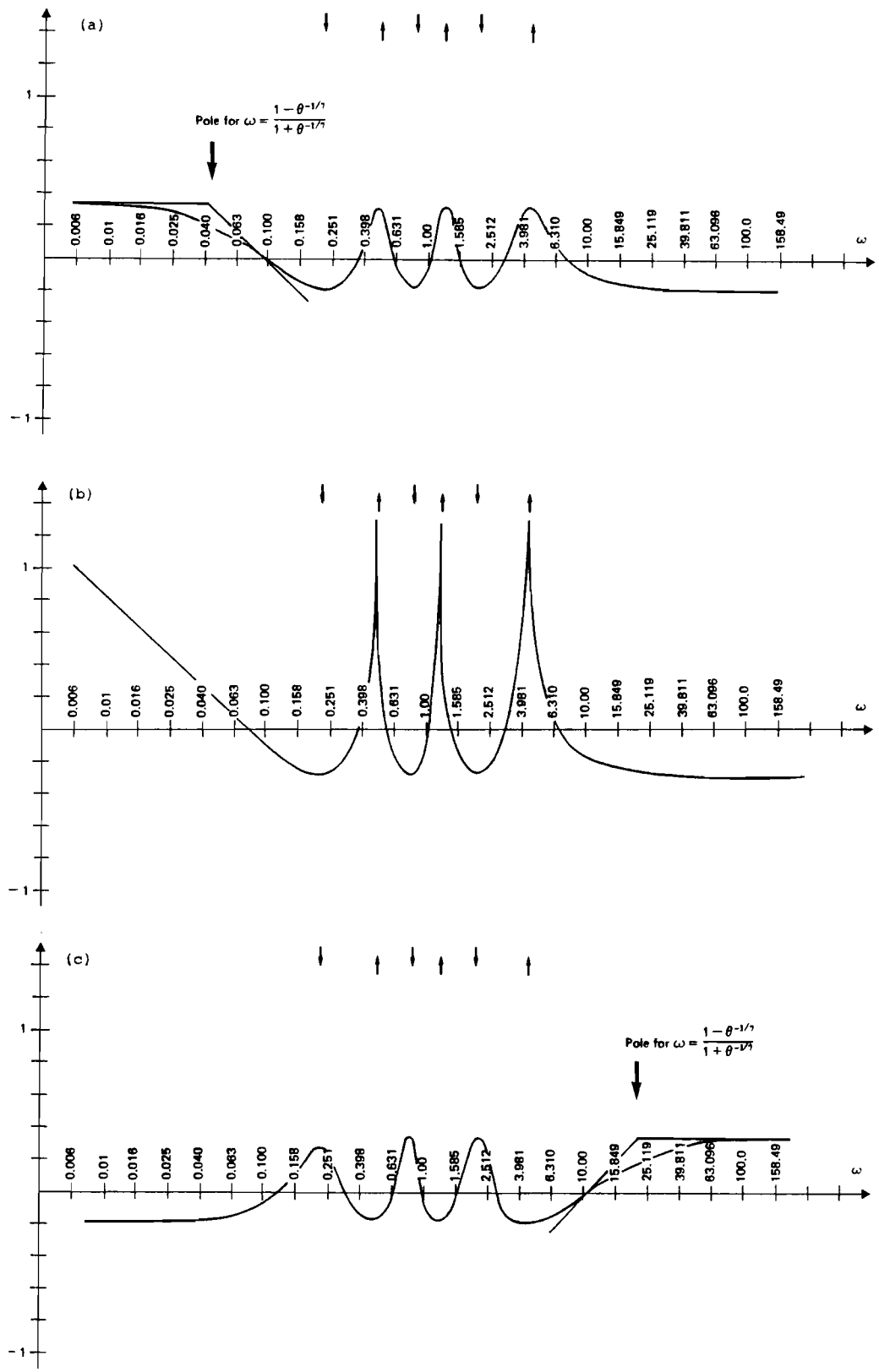

FIGURE 10 Bode plots for a seasonal difference operator (periodicity 7): (a) ϑ=0.55; (b) ϑ=0.95; (c) ϑ=−0.55.

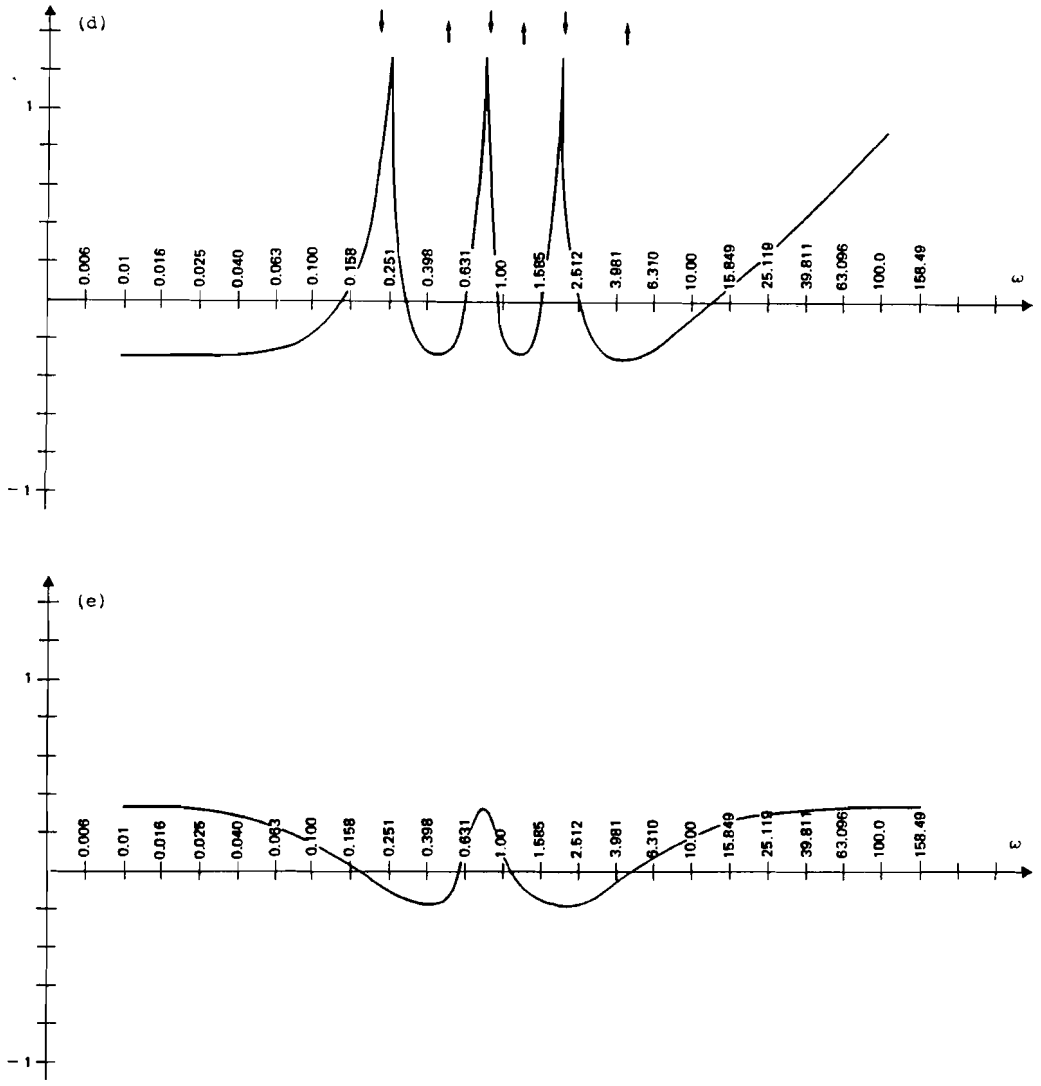

FIGURE 10 (continued) Bode plots for a seasonal difference operator (periodicity 7): (d) $\vartheta=-0.95$; (e) $\vartheta=-0.55$.

investigated. According to Figure 2, if we replace frequency ω by 2 arc tan ω we will obtain the spectrum of the modified transfer function; a standard chart has been designed especially to aid in this task (see Figure 12). The basic steps of the identification procedure are as follows :

1. Calculate the spectral density function and plot it on the special chart.

2. Try to make a piecewise-linear approximation of this function, bearing in mind the results obtained in Section 3 (i.e., the slopes of the lines can be $\pm 1, \pm 2 \ldots$). The peaks on the plot should be treated with special care, as

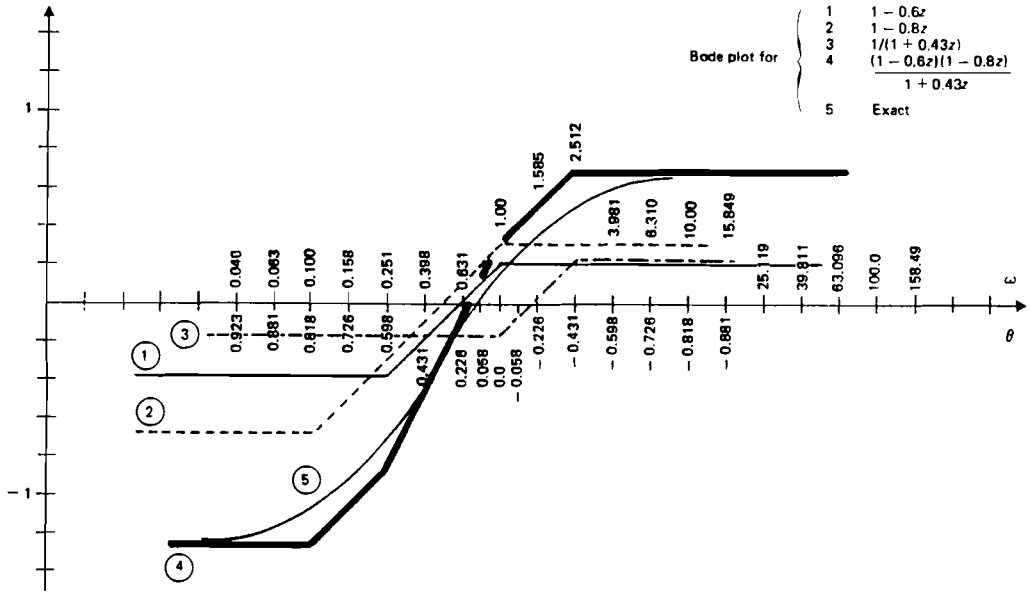

FIGURE 11 Construction of a Bode plot for a general ARMA model.

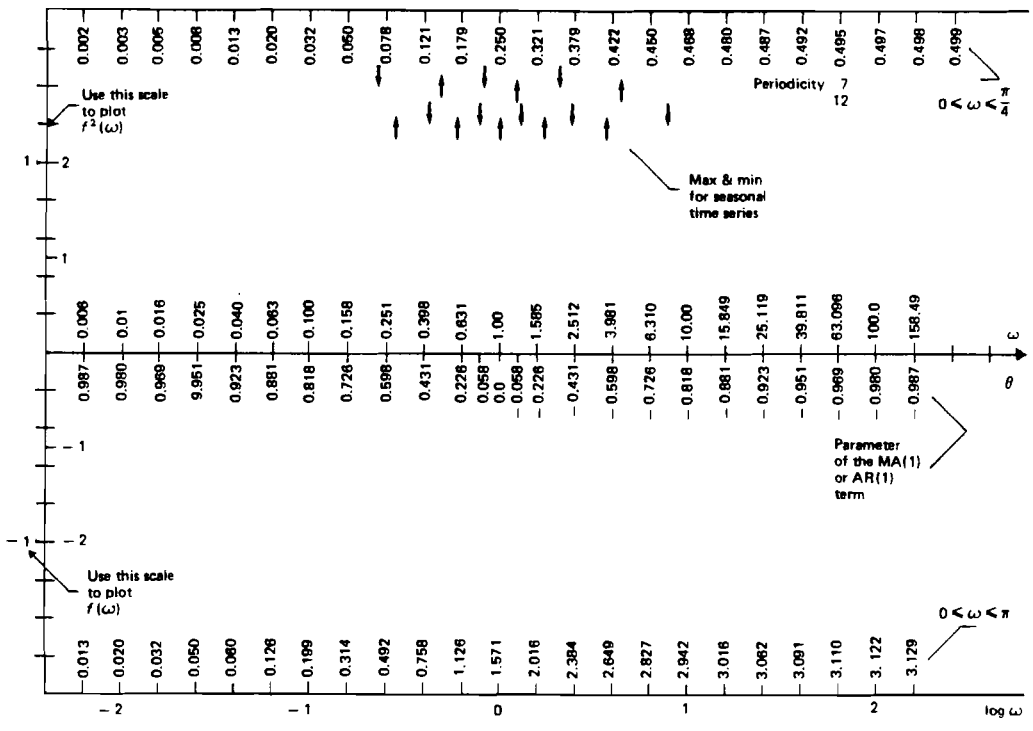

FIGURE 12 A standard chart for plotting the linearized spectral density function.

should possible seasonal patterns.

3. Using the asymptotic decomposition obtained in the previous step, determine the positions of the zeros and poles of the modified transfer function $g(\lambda)$.

4. Transform every zero and pole from the λ complex plane to the z plane; this gives us the transfer function $G(z)$.

We should point out that, in principle, this procedure gives us parameter values for a model of any complexity. Experiments have also shown that this method is surprisingly accurate — the typical error in parameter determination is about 10–20%. It is almost impossible to obtain results of the same accuracy from analysis of the autocorrelation function.

Of course, to use this procedure requires some feeling for what the frequency response means, and this can only be gained through experience. The appropriate approximation must be found by trial and error; in many cases the solution is not unique and in others the method does not work. But the fundamental idea behind this approach is that time series can be analyzed in some depth using only a pencil, a piece of paper and a pocket calculator.

To clarify this approach further, and to illustrate its possibilities and limitations, we will now present a number of examples together with a detailed description of the corresponding analyses.

4.1. Simulated Time Series

Three experiments were performed in each case. The length of the time series generated in each run was 200; the standard deviation of the noise was 1%. Three methods of spectrum estimation were used: the maximum entropy method (ARSPEC) (Beamish and Priestley, 1981), the G-transform approach (GSPEC) (Gray, Houston and Morgan, 1978), and the standard Bartlett window

method (BT) (Jenkins and Watts, 1968).

Example 1 (Figure 13). In this case we tried to identify an MA(1) model with $\vartheta = 0.95$. The ARSPEC estimate gives a very clear result — it is obvious that the piecewise-linear approximation is very accurate. The estimated value of the parameter is 0.881, which leads to an error of approximately 8% .

The situation is not so good for the GSPEC estimate — the spectrum behaves quite randomly at low frequencies. For this reason it is virtually impossible to determine the exact value of the coefficient, although it seems almost certain that there is a pole for $\omega = 1$, and therefore this model must contain an MA(1) component.

Example 2. In this example we generated time series using an MA(1) model with $\vartheta = -0.95$. On looking at the spectral density function it is possible to conclude that the investigated time series has MA(1) structure with parameter ϑ between −0.881 and −0.923 (see Figure 14), which is rather a good result. The behavior of the ARSPEC estimate was not very good at low frequencies, although it was still possible to plot the horizontal asymptote. The accuracy of the coefficient was also acceptable — we obtained a value of approximately −0.85.

However, more accurate analysis of the Bode plot shows that the transfer function has a pole not for $\omega = 1$ but for $\omega \simeq 1.25$, and thus the time series was generated by an ARMA(1,1) model with parameters −0.893 and −0.06. The small value of the AR parameter suggests that it can be neglected. It is not yet known how to formulate and verify this hypothesis statistically, but an analysis of the confidence limits of the spectrum may be helpful (see Figure 15). This analysis was performed for the BT spectrum estimate illustrated in Figure 14(b). This figure suggests that the MA(1) model should be accepted. It is quite clear why the AR part was detected — the sample ACF corresponds to an

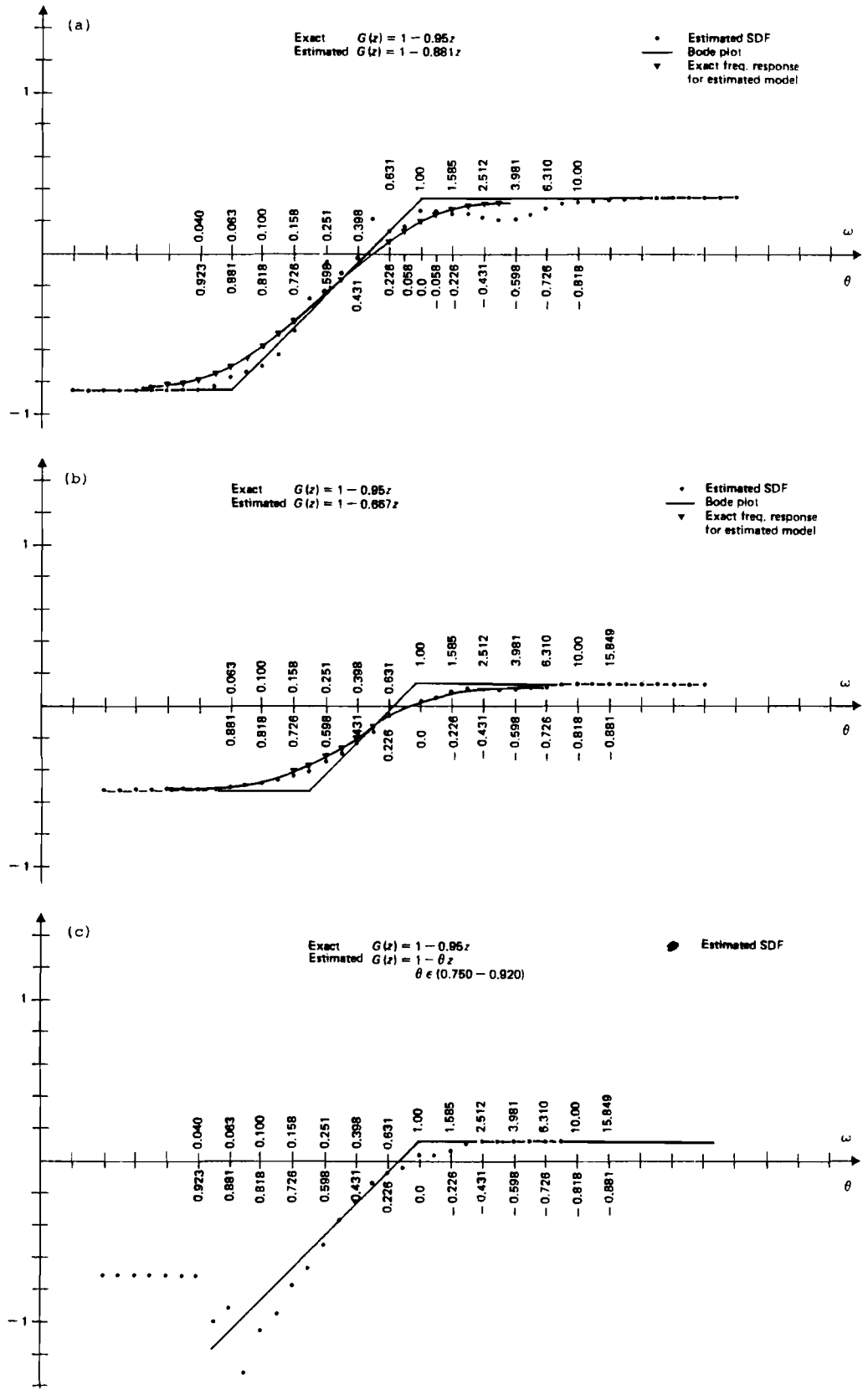

FIGURE 13 Bode plot for simulated MA(1) time series with $\vartheta = 0.95$: (a) ARSPEC estimate; (b) BT estimate; (c) GSPEC estimate.

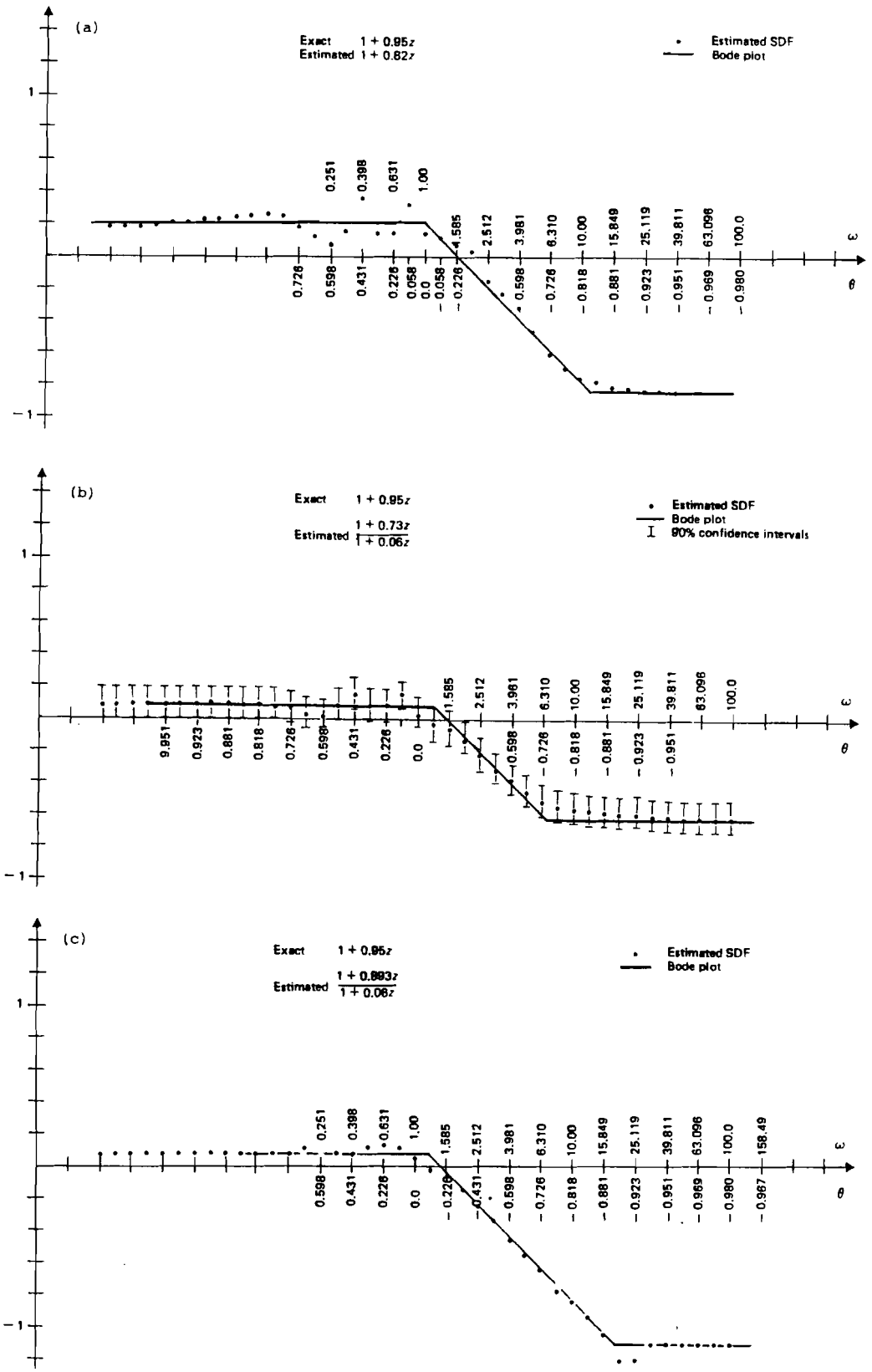

FIGURE 14 Bode plots for simulated MA(1) time series with $\vartheta=-0.95$: (a) ARSPEC estimate; (b) BT estimate with confidence intervals; (c) GSPEC estimate.

ARMA rather than to an MA model (Figure 16).

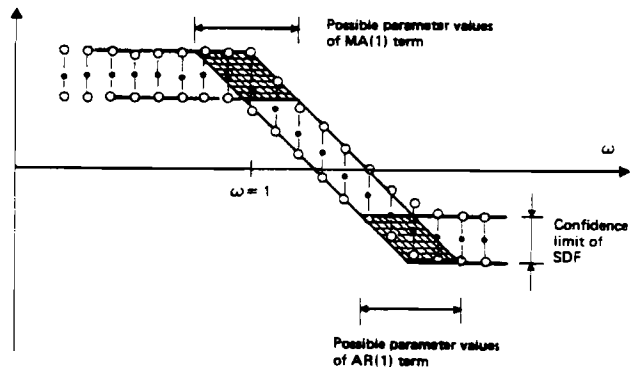

FIGURE 15 Possible parameter values for an MA(1) model — analysis of confidence intervals.

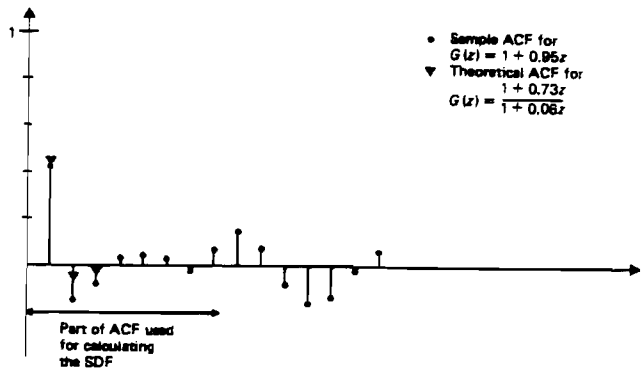

FIGURE 16 Sample ACF for simulated MA(1) time series (length of time series = 200).

Example 3. In this example the situation is more complicated. Our first conclusion is that there is a peak on the frequency response plot. Is it reasonable to expect complex roots? The answer is yes — we can assume that there is a complex root for $\omega_r \simeq 0.05$. However, to compensate for the slope which is generated by such a root we must add an additional zero for $\omega \simeq 0.5$. In order to ensure that the frequency response has the proper shape for large values of ω we must also add a zero for $\omega \simeq 10$. Using formula (49), we can estimate the value of the damping factor — this is approximately 0.9. We now try to plot the exact frequency response, as shown in Figure 17(a). The identified model has

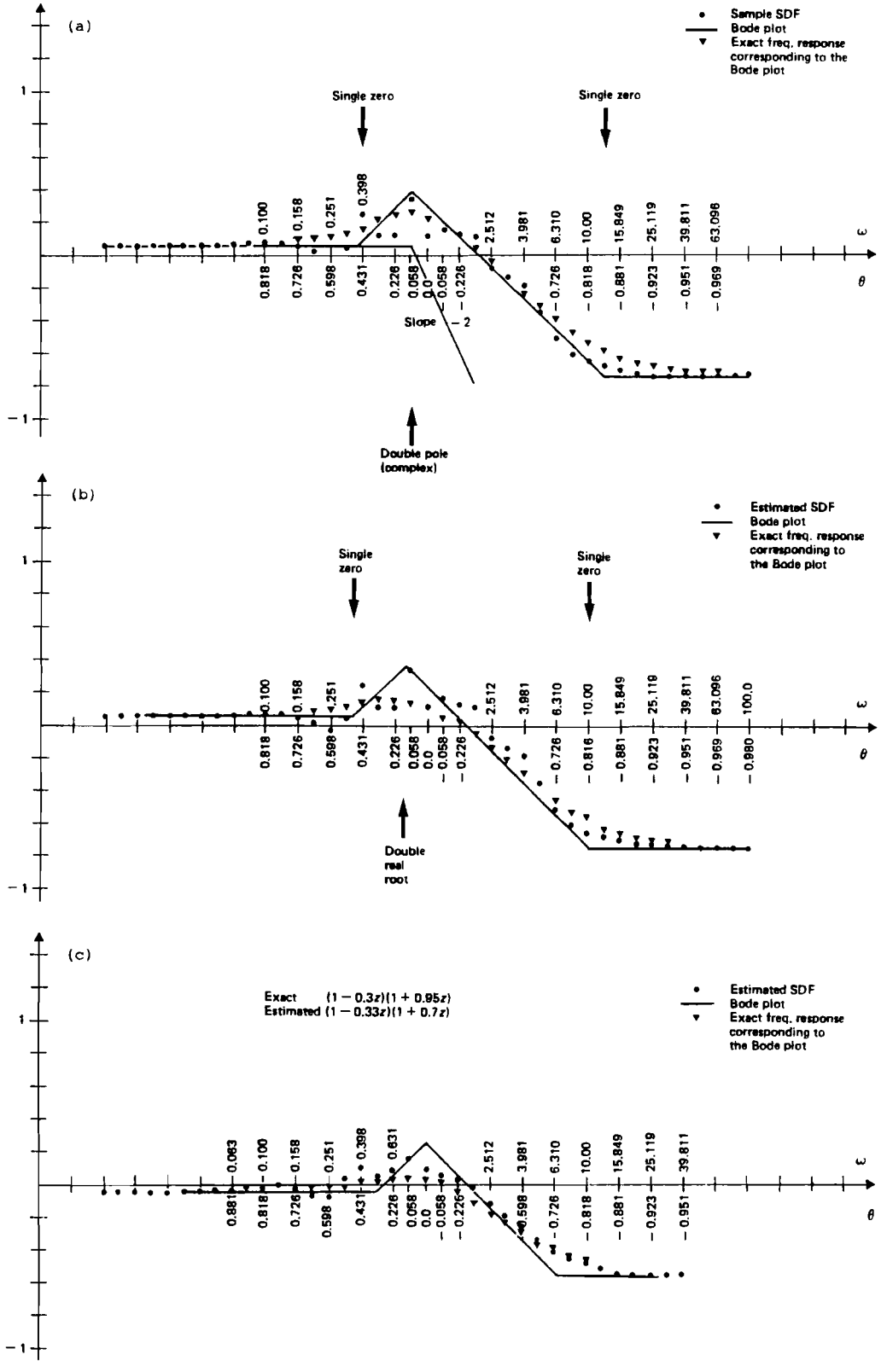

FIGURE 17 Bode plots for simulated MA(2) time series: (a) Investigation of the hypothesis that for $\omega \simeq 0.5$ the transfer function of the model has a pair of conjugate complex roots, ARSPEC estimate; (b) Investigation of the hypothesis that for $\omega \simeq 0.5$ the transfer function of the model has a pair of double real roots, ARSPEC estimate; (c) BT estimate.

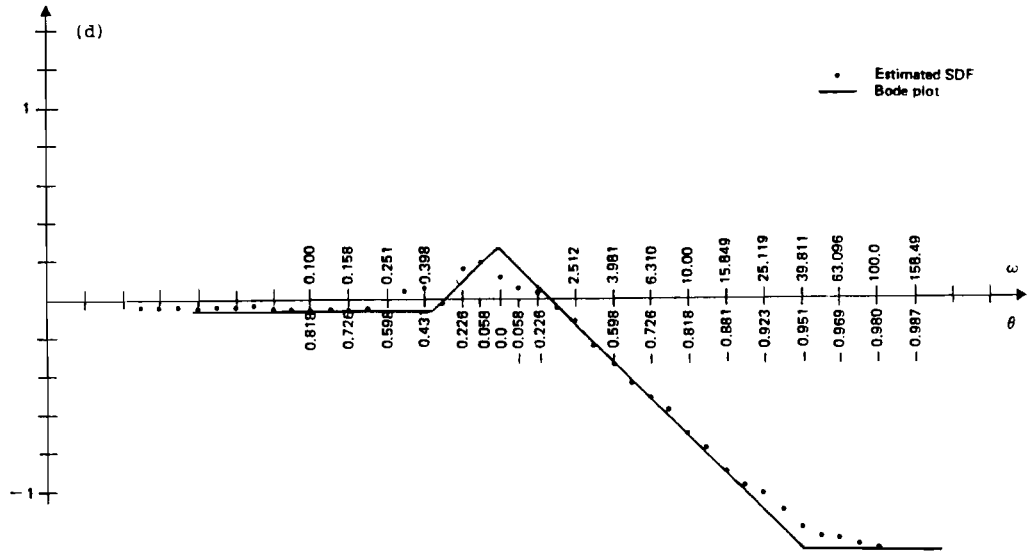

FIGURE 17 (continued) Bode plots for simulated MA(2) time series: (d) GSPEC estimate.

the following form:

$$G(z) = \frac{(1-0.467z)(1+0.853z)}{(1-0.241z+0.066z^2)} . \tag{79}$$

A similar result can be obtained from the GSPEC estimate (Figure 17d), the only difference lying in the value of one of the coefficients (0.95 instead of 0.85).

We should point out that another hypothesis can be put forward — that there is one double real root for $\omega = 0.794$ rather than a pair of complex roots. Figure 17(b) shows that this hypothesis can also be accepted; the resulting model has the following transfer function:

$$G(z) = \frac{(1-0.467z)(1+0.858z)}{(1-0.115z)^2} . \tag{80}$$

When we apply the same procedure to BT and GSPEC estimates we obtain an MA(2) model (Figure 17c). Because of the rather poor behavior of the sample spectral density function (SDF) for frequencies around zero, it is difficult to determine which model gives us the best fit. As in the previous example, the sample ACF corresponds to the ARMA rather than to the second-order MA

model with parameters $\vartheta_1 = 0.3$ and $\vartheta_2 = -0.6$.

Example 4. The Bode plot for this case is presented in Figure 18 (only the ARSPEC estimate is shown). It may be observed that this is similar to the Bode plot analyzed in the previous example, except that the peak is more pronounced in this case. Reasoning similar to that used in the previous example shows that the best fit will be obtained if we assume a double root for $\omega = 1$. This leads to the transfer function

$$G(z) = (1-0.6z)(1+0.81z) \ , \tag{81}$$

which corresponds very well to the exact model with $\vartheta_1 = 0.6$ and $\vartheta_2 = -0.95$. The structure of the model is the same as in the previous example, but the accuracy of the identification is better in this case.

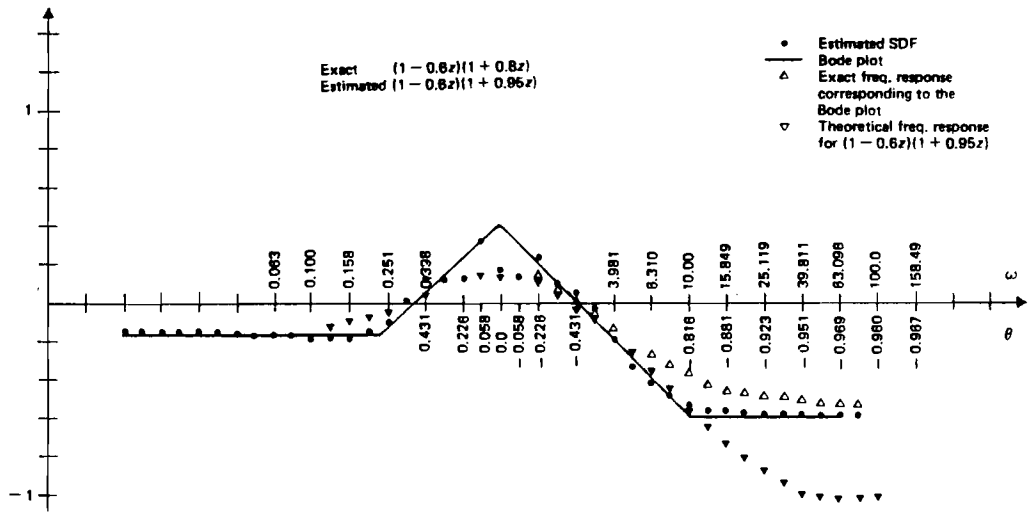

FIGURE 18 Bode plot for simulated MA(2) time series, ARSPEC estimate (Example 4).

The reason for this increased accuracy is obvious — the method works better when the distance between roots (or poles) is large. For this reason we should not expect the method to give good results when the coefficients have almost equal values, say 0.6 and 0.8. However, even in this situation the results are not bad. This is illustrated in the next example.

Example 5. In this example we analyze the time series generated by the MA(2) model

$$G(z) = (1 - 0.6z)(1 - 0.8z) \ . \tag{82}$$

It follows immediately that we will obtain a reasonable fit for the following transfer function:

$$G(z) = (1 - 0.715z)^2 \ . \tag{83}$$

It is impossible to detect that in this case the transfer function has two different roots —the theoretical and estimated Bode plots practically coincide (Figure 19). The ACF is more informative in this case. This seems to be generally true for pure MA processes; for more complex cases in which the pattern of the ACF is not so obvious the spectral method should work better. This situation is considered in the next example.

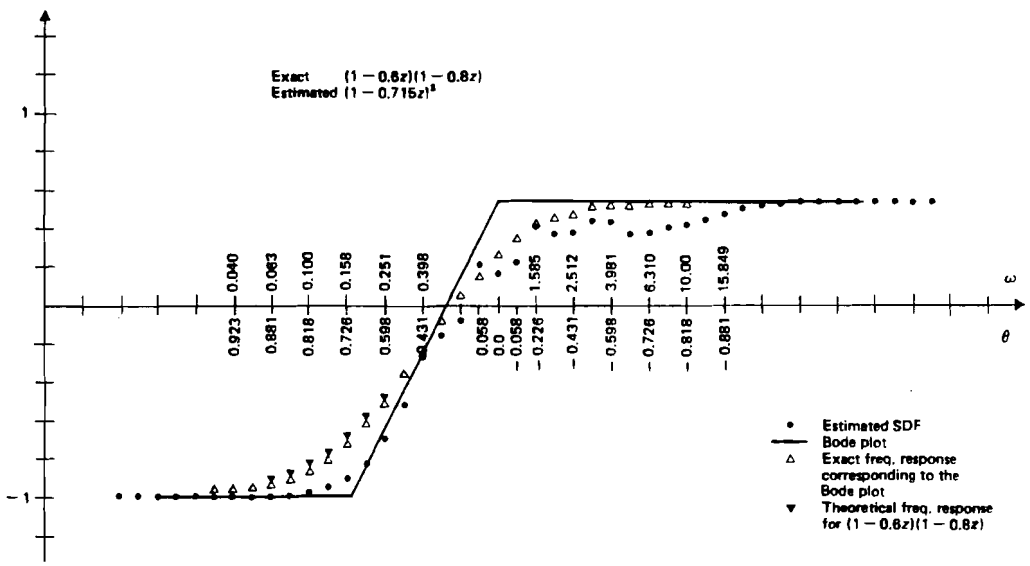

FIGURE 19 Bode plot for simulated MA(2) time series, ARSPEC estimate (Example 5).

Example 6. This is Example 1 from Gray, Kelley and McIntire (1978). The shape of the Bode plot is similar to that considered in previous examples, but

the whole plot is shifted to the left. Reasoning as in Example 3, we obtain the results presented in Figure 20. We observe the strong influence of the factor with complex roots. The identified model has the following transfer function:

$$G(z) = \frac{(1-0.715z)(1-0.115z)}{1-1.127z+0.602z^2} . \tag{84}$$

This is not a bad result when compared with the exact model

$$G(z) = \frac{1-0.8z}{1-1.36z+0.68z^2} . \tag{85}$$

In this case the ACF pattern is very complicated and it is not easy to identify the model on the basis of this information alone.

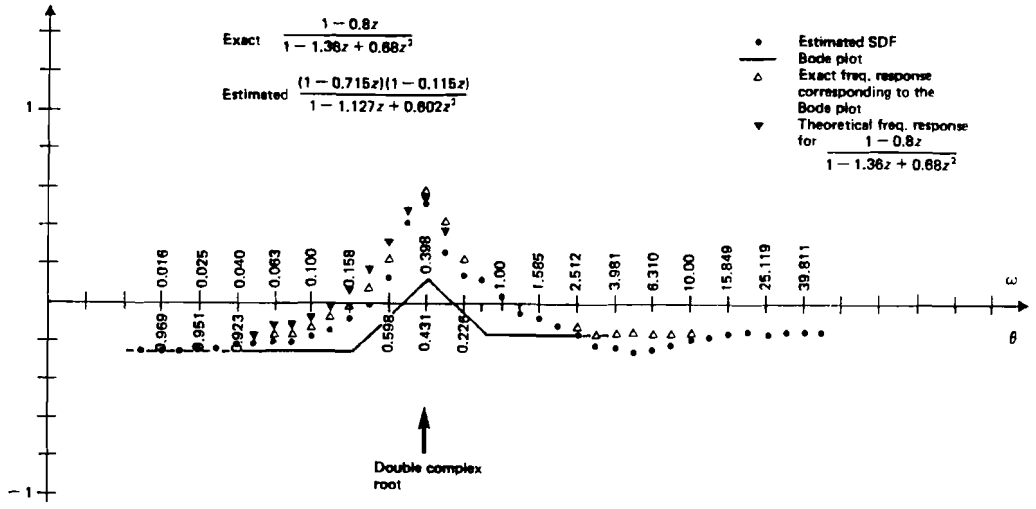

FIGURE 20 Bode plot for simulated ARMA(2,1) time series, ARSPEC estimate (Example 6).

Example 7. In this example it is again not very easy to identify the model by analyzing the ACF (Figure 21). The ACF oscillates; it is not possible to detect the presence of an MA term. However, the situation is clearer in the frequency domain — after simple analysis we obtain

$$G(z) = \frac{(1-0.65z)^2}{1+0.63z} . \tag{86}$$

This is a good approximation of the real model

$$G(z) = \frac{(1-0.8z)(1-0.3z)}{1+0.6z} . \tag{87}$$

The Bode plots for this example are presented in Figure 21(b).

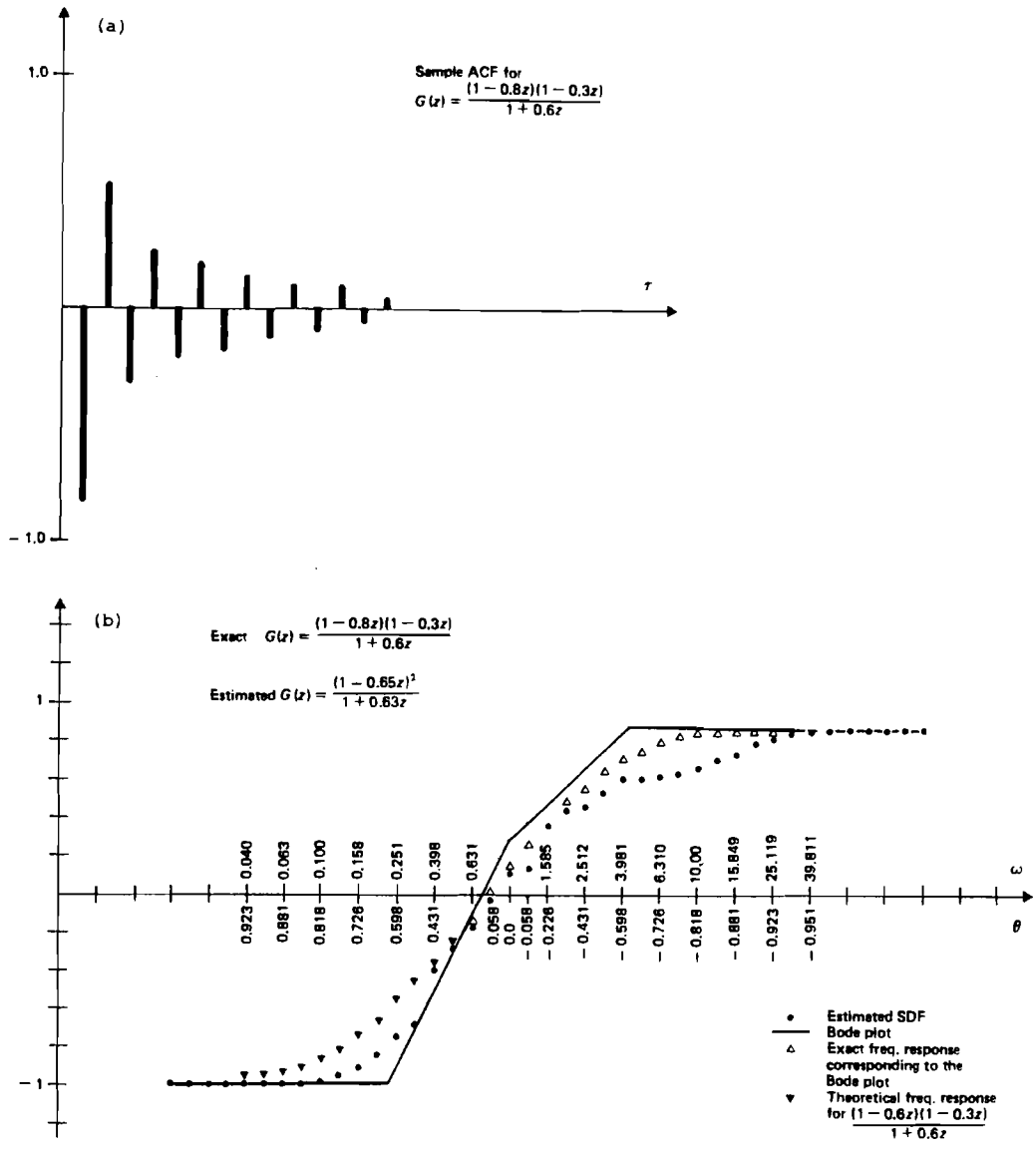

FIGURE 21 (a) Sample ACF for time series from Example 7; (b) Bode plot for simulated ARMA(2,1) time series, ARSPEC estimate (Example 7).

4.2. Box–Jenkins Time Series

Example 8. Let us analyze series A from Box and Jenkins (1970). Figure 22(a–f) presents the results of spectral analysis, i.e., frequency responses and asymptotic approximations for the original and differenced time series. Three methods were used for estimating the spectrum —ARSPEC, GSPEC and BT. The results are summarized in Table 1.

TABLE 1. Identification of series A from Box and Jenkins (1970) using different spectrum estimation methods.

Spectrum estimation method	Model
ARSPEC	$\frac{1-0.312z}{1-0.785z}$
ARSPEC (differenced)	$\frac{1-0.73z}{(1-0.116z)(1-z)}$
GSPEC	$\frac{1-0.43z}{1-0.865z}$
GSPEC (differenced)	$\frac{1-0.77z}{1-z}$
BT	$\frac{1-0.798z}{1-0.33z}$
BT (differenced)	$\frac{1-0.654z}{1-z}$
Box–Jenkins	$\frac{1-0.58z}{1-0.92z}$ $\frac{1-0.72z}{1-z}$

Example 9. In this example we analyze series B from Box and Jenkins (1970). The same runs were performed as in Example 8; the results are given in Table 2 and Figure 23.

In this case the GSPEC estimate evidently gives the wrong result; the reason probably lies in the trend in the data. The results are compared with the model estimated using the MINITAB package because there seems to be a mistake in the Box–Jenkins book.

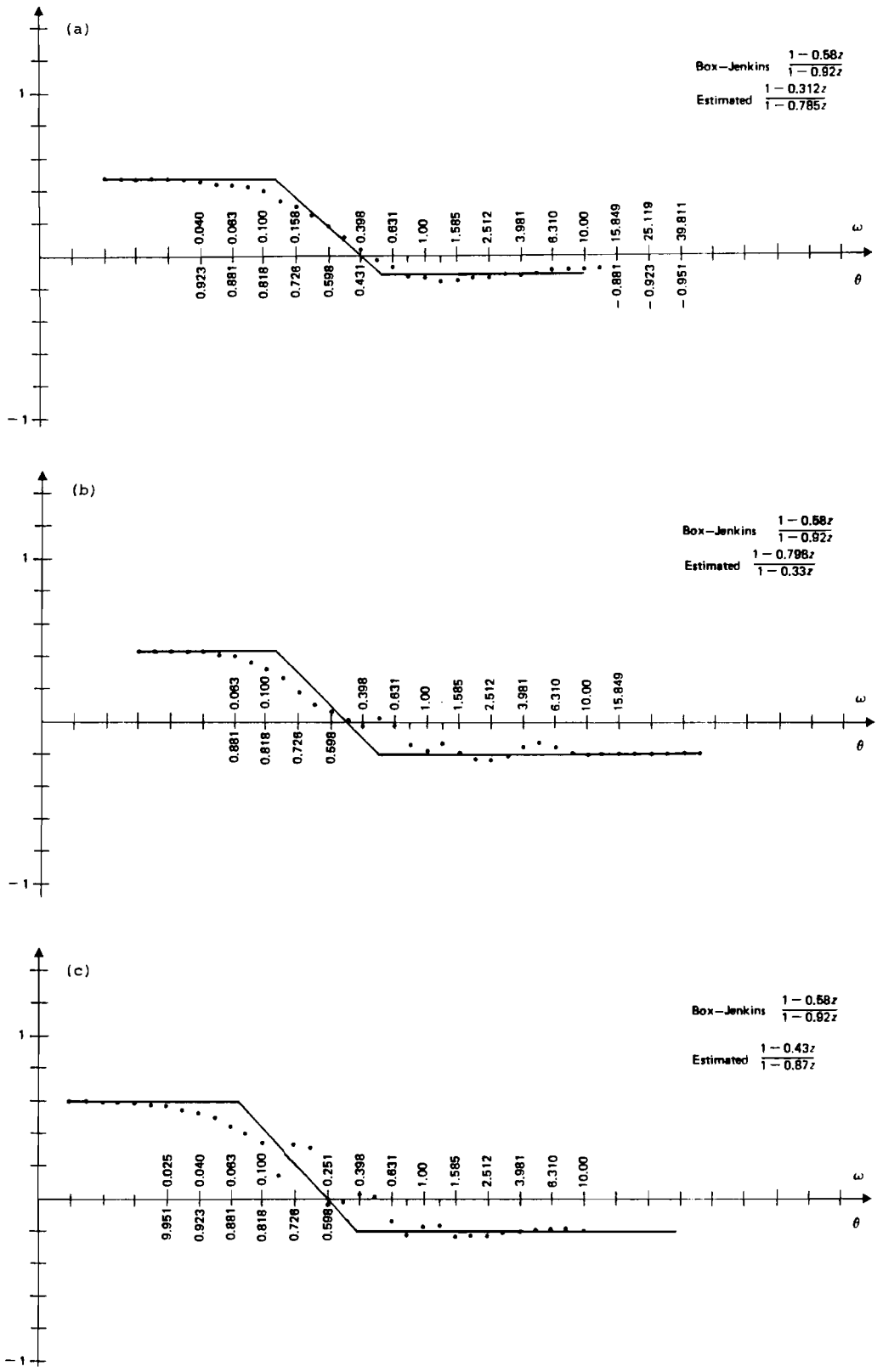

FIGURE 22 Bode plots for time series A from Box and Jenkins: (a) ARSPEC estimate; (b) BT estimate; (c) GSPEC estimate.

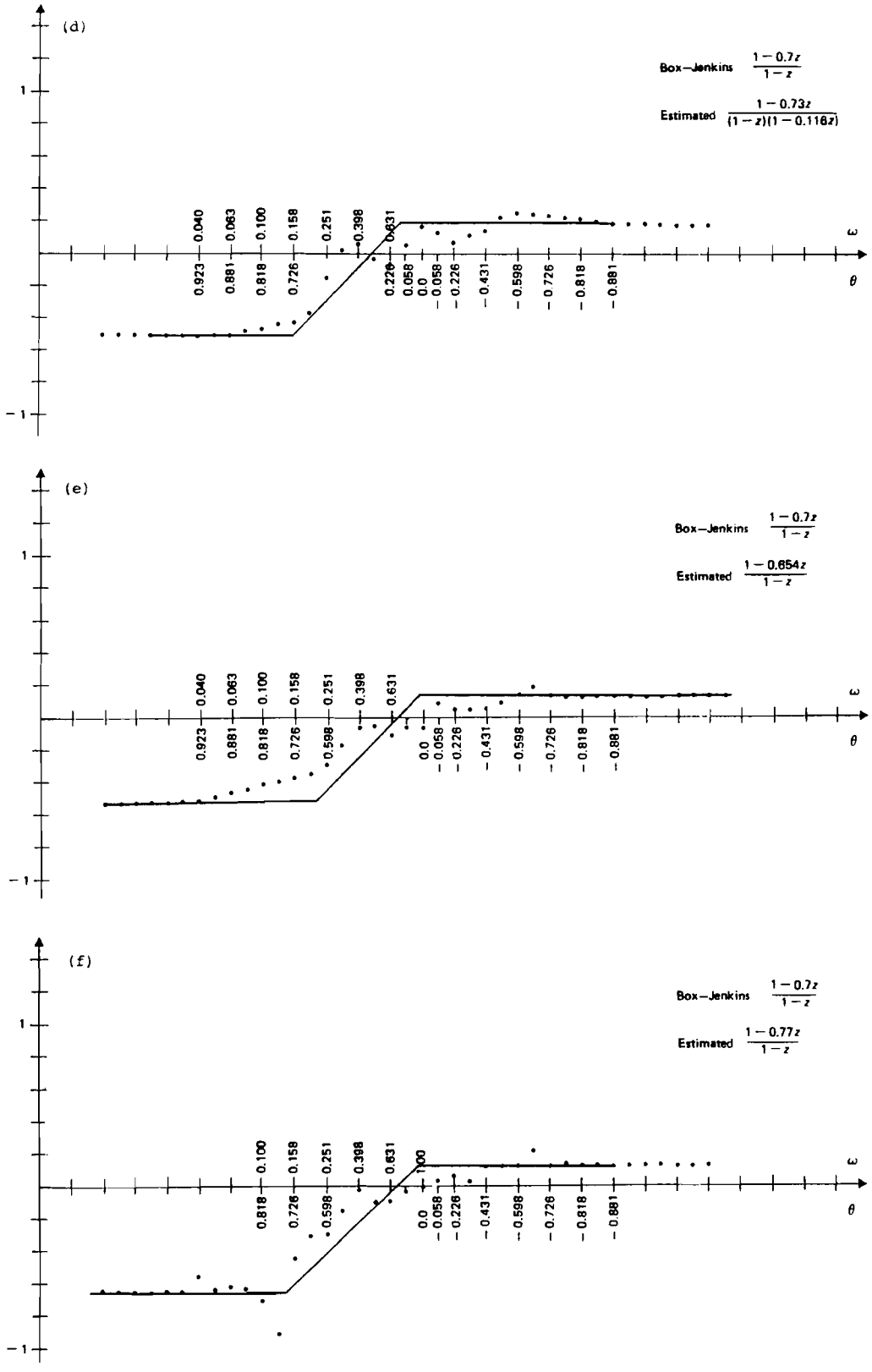

FIGURE 22 (continued) Bode plots for time series A from Box and Jenkins: (d) ARSPEC estimate, differenced data; (e) BT estimate, differenced data; (f) GSPEC estimate, differenced data.

TABLE 2. Identification of series B from Box and Jenkins (1970) using different spectrum estimation methods.

Spectrum estimation method	Model
ARSPEC	$\frac{1-0.586z}{1-z}$
ARSPEC (differenced)	$\frac{1-0.6z}{1-z}$
GSPEC*	?
GSPEC (differenced)	$\frac{1-0.598z}{1-z}$
BT*	?
BT (differenced)	$\frac{1-0.519z}{(1-0.092z)(1-z)}$
Estimated model**	$\frac{1-0.61z}{1-z}$

* Unacceptable result. **Using MINITAB package.

Example 10. Here we look at series C from Box and Jenkins (1970). The results obtained using our standard procedure are presented in Figure 24 and Table 3.

TABLE 3. Identification of series C from Box and Jenkins (1970) using different spectrum estimation methods.

Spectrum estimation method	Model
ARSPEC	$\frac{1+0.226z}{(1-z)^2}$
ARSPEC (differenced)	$\frac{1}{(1-0.77z)(1-z)}$
GSPEC	$\frac{(1-0.25z)^2}{(1-0.85z)^2}$
GSPEC (differenced)	$\frac{1}{(1-0.798z)(1-z)}$
BT	$\frac{(1-0.248z)^2}{(1-0.776z)^2}$
BT (differenced)	$\frac{1}{(1-0.726z)(1-z)}$
Box–Jenkins	$\frac{1}{(1-0.82z)(1-z)}$ $\frac{(1-0.417z)(1+0.287z)}{(1-z)^2}$

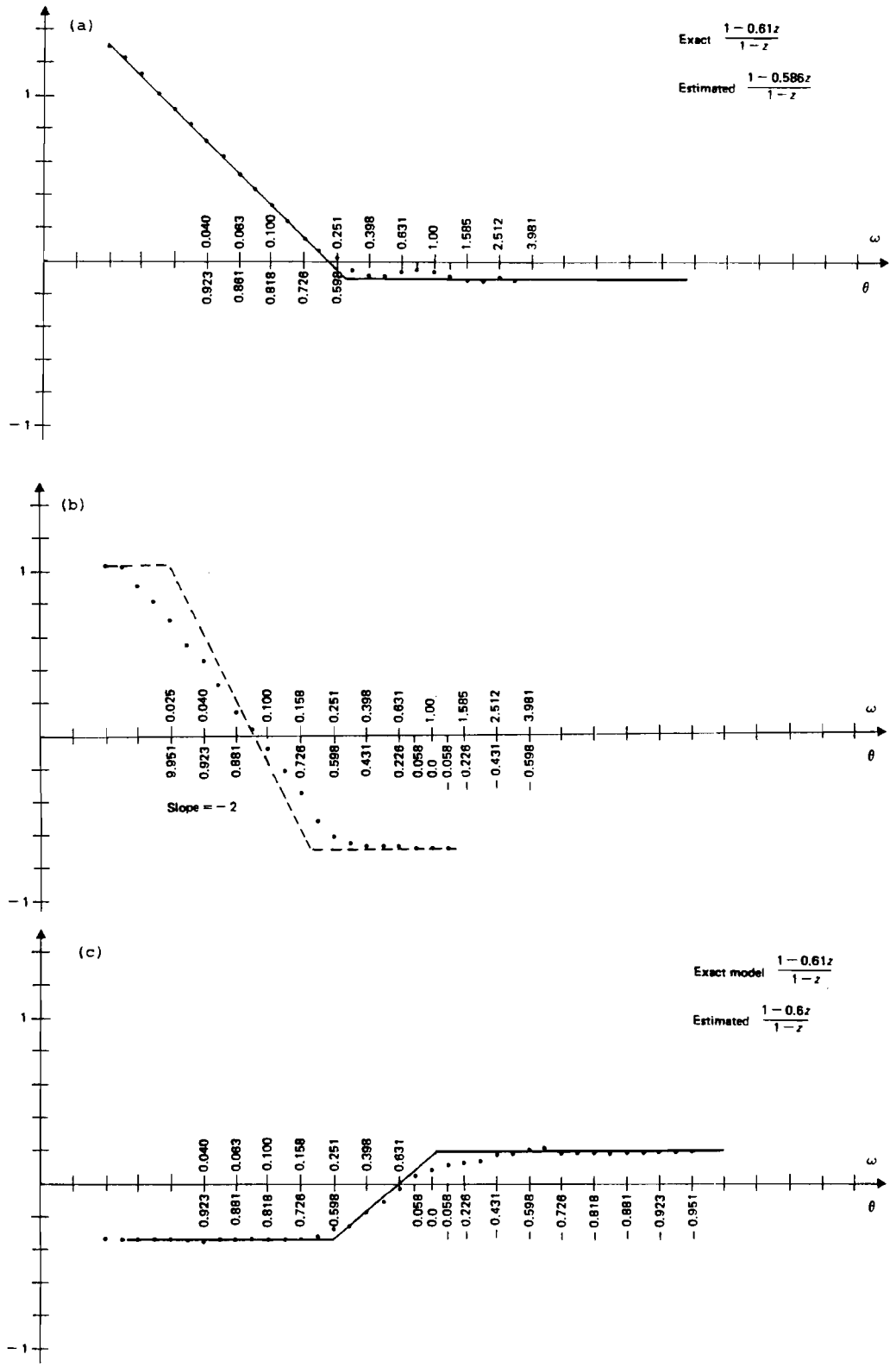

FIGURE 23 Bode plots for time series B from Box and Jenkins: (a) ARSPEC estimate; (b) GSPEC estimate; (c) ARSPEC estimate, differenced data.

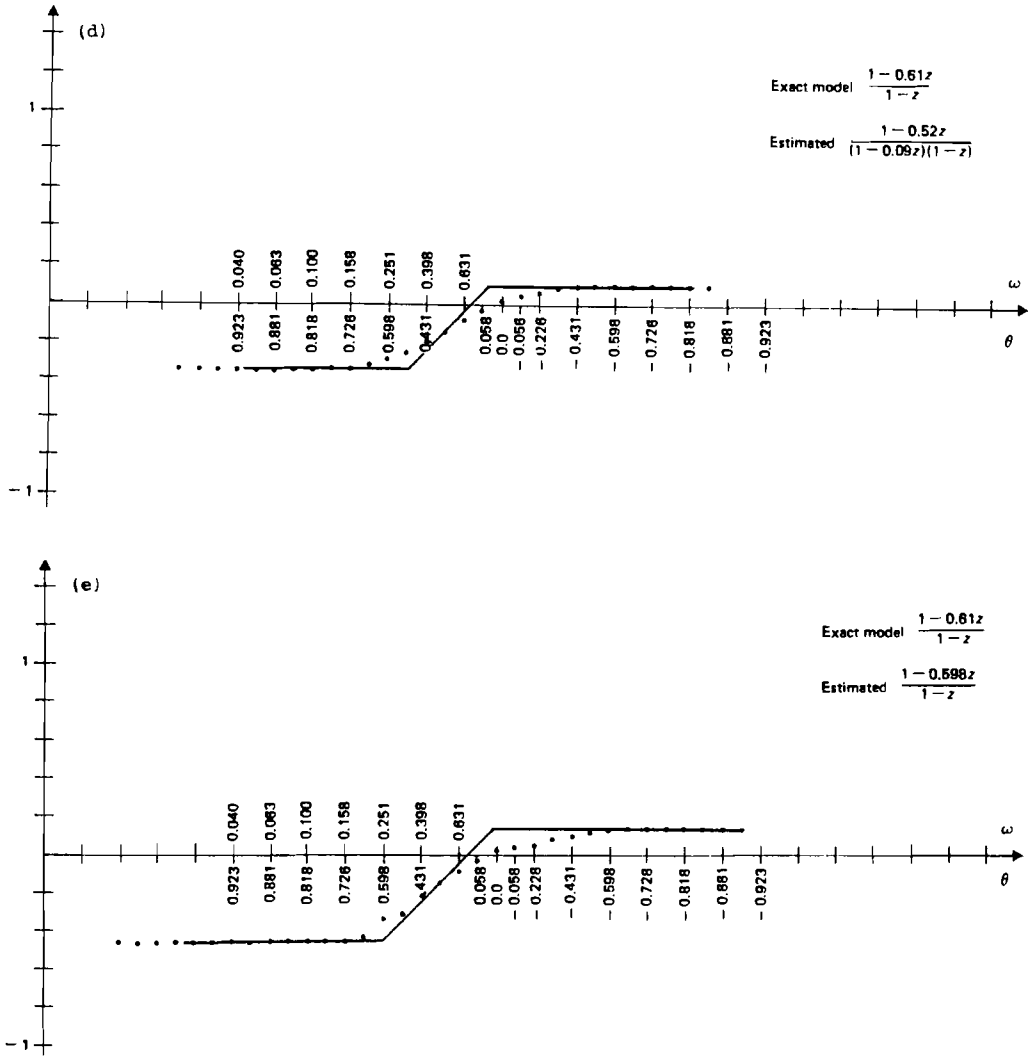

FIGURE 23 (continued) Bode plots for time series B from Box and Jenkins: (d) BT estimate, differenced data; (e) GSPEC estimate, differenced data.

The results obtained for the AR model with single differenced data are very good. The only major discrepancy arises for the MA model with double differenced data. It is rather difficult to explain the source of this problem — it is probably caused by a trend in the non-differenced time series.

Example 11. This is concerned with series D from Box and Jenkins (1970). The results are presented in Figure 25(a–f) and Table 4.

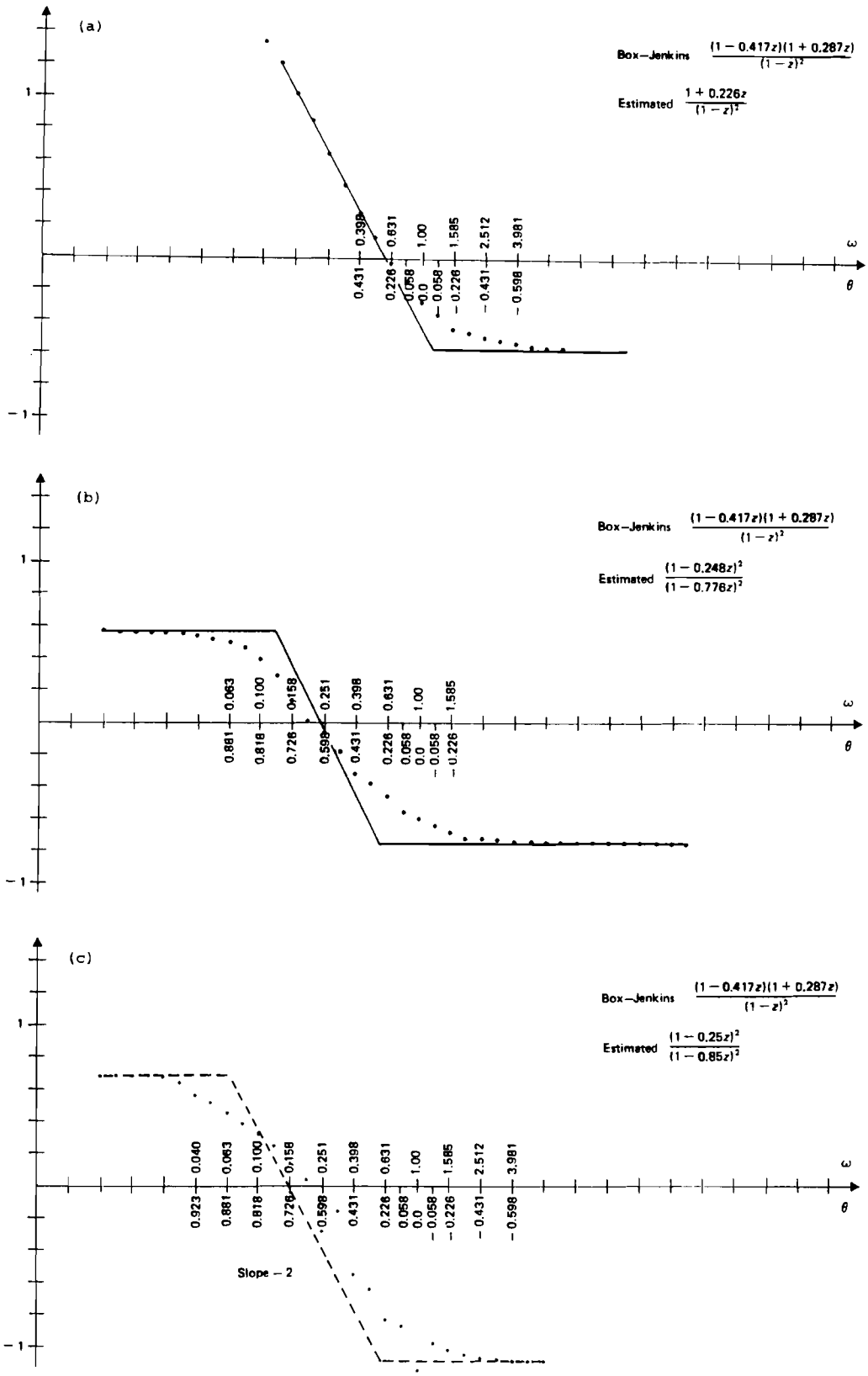

FIGURE 24 Bode plots for time series C from Box and Jenkins: (a) ARSPEC estimate; (b) BT estimate; (c) GSPEC estimate.

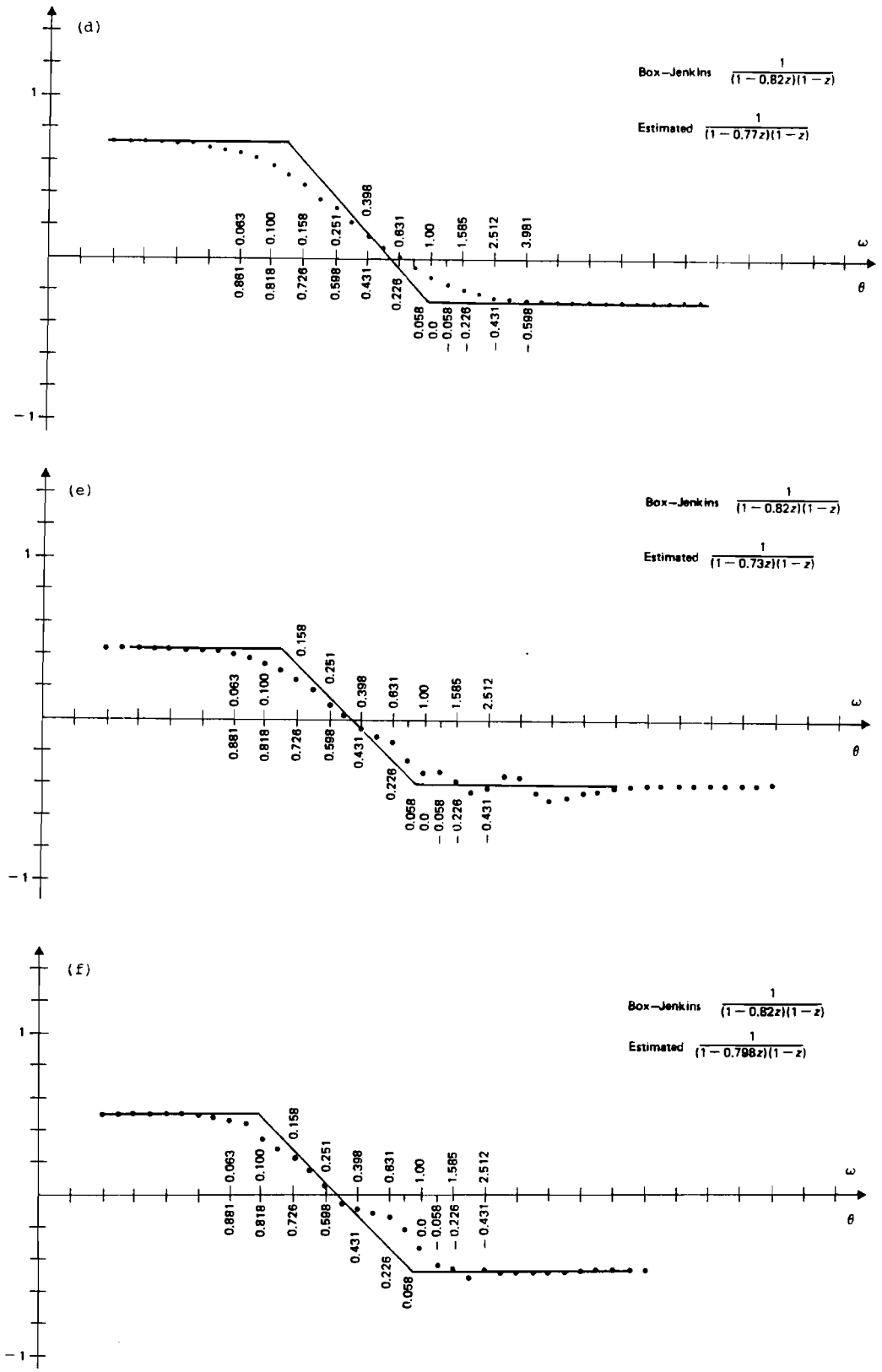

FIGURE 24 (continued) Bode plots for time series C from Box and Jenkins: (d) ARSPEC estimate, differenced data; (e) BT estimate, differenced data; (f) GSPEC estimate, differenced data.

TABLE 4. Identification of series D from Box and Jenkins (1970) using different spectrum estimation methods.

Spectrum estimation method	Model
ARSPEC	$\frac{1}{1-0.891z}$
ARSPEC (differenced)	$\frac{1}{(1+0.04z)(1-z)}$
GSPEC	$\frac{1}{1-0.853z}$
GSPEC (differenced)	?
BT	$\frac{1}{1-0.81z}$
BT (differenced)	$\frac{1-0.667z}{(1-0.552z)(1-z)}$
Box–Jenkins	$\frac{1}{1-0.87z}$ $\frac{1-0.06z}{1-z}$

Once again we obtained uninterpretable results for GSPEC. Note also that it is quite difficult to interpret the spectrum for differenced data, the main reason being the small value of the zero (or pole). However, the spectral responses of the identified model and the second Box–Jenkins model are almost the same. It is impossible to conclude from Figure 25(d) whether the frequency response has a zero or pole for $\omega = 1$; in the author's opinion it is a zero, but because of possible inaccuracies in the estimation of the spectrum not too much confidence should be placed in this conclusion.

Example 12. This is based on series E from Box and Jenkins (1970), the Wolfer sunspot number series. The frequency response of this famous time series is presented in Figure 26(a) (ARSPEC estimate). Using the approximation shown in this diagram we obtain the following model:

$$G(z) = \frac{(1-0.68z)^2(1+0.431z)}{(1-0.93z)(1-1.53z+0.87z^2)} . \tag{88}$$

A similar result can be obtained using the BT estimate:

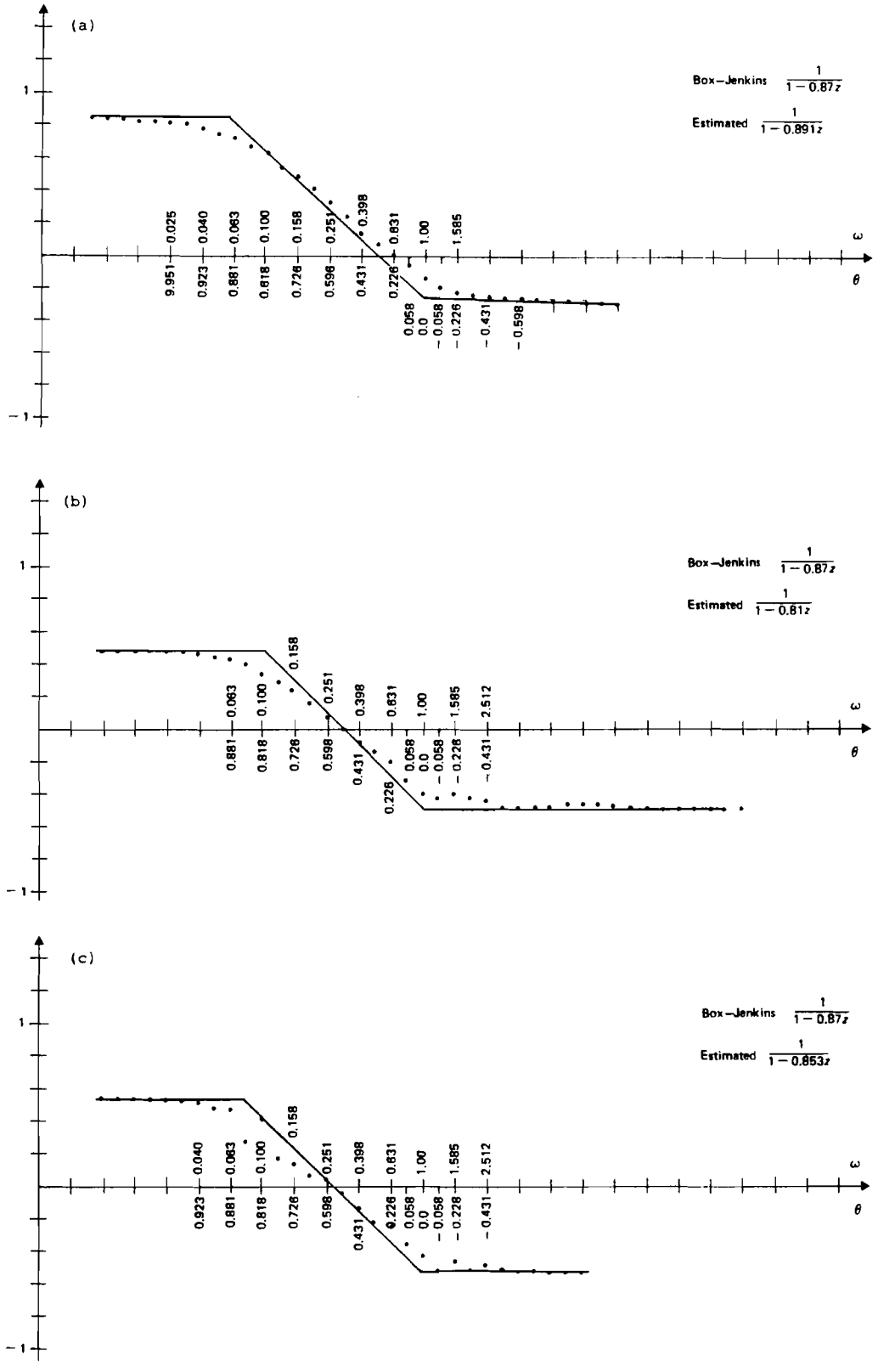

FIGURE 25 Bode plots for time series D from Box and Jenkins: (a) ARSPEC estimate; (b) BT estimate; (c) GSPEC estimate.

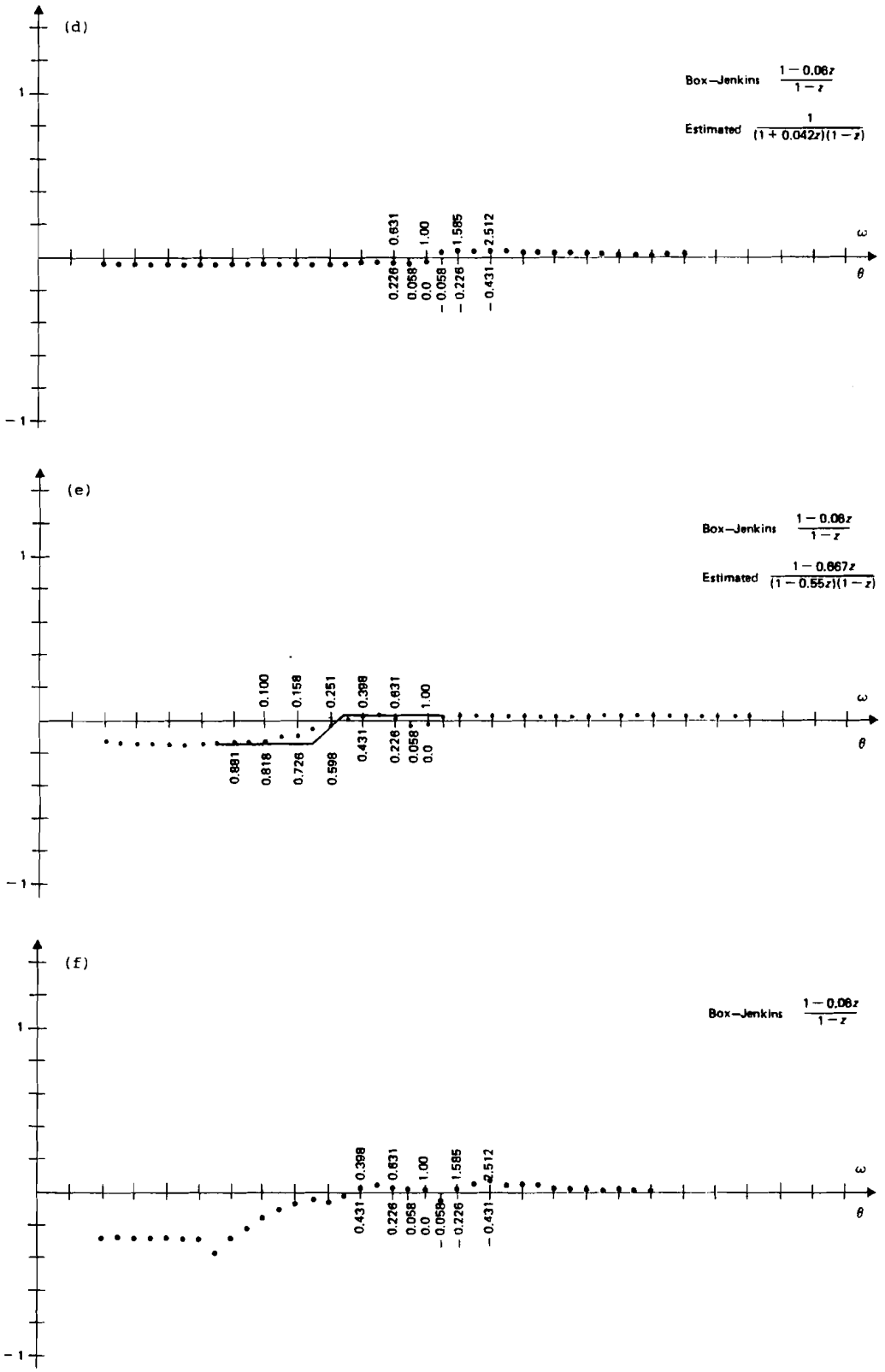

FIGURE 25 (continued) Bode plots for time series D from Box and Jenkins: (d) ARSPEC estimate, differenced data; (e) BT estimate, differenced data; (f) GSPEC estimate, differenced data.

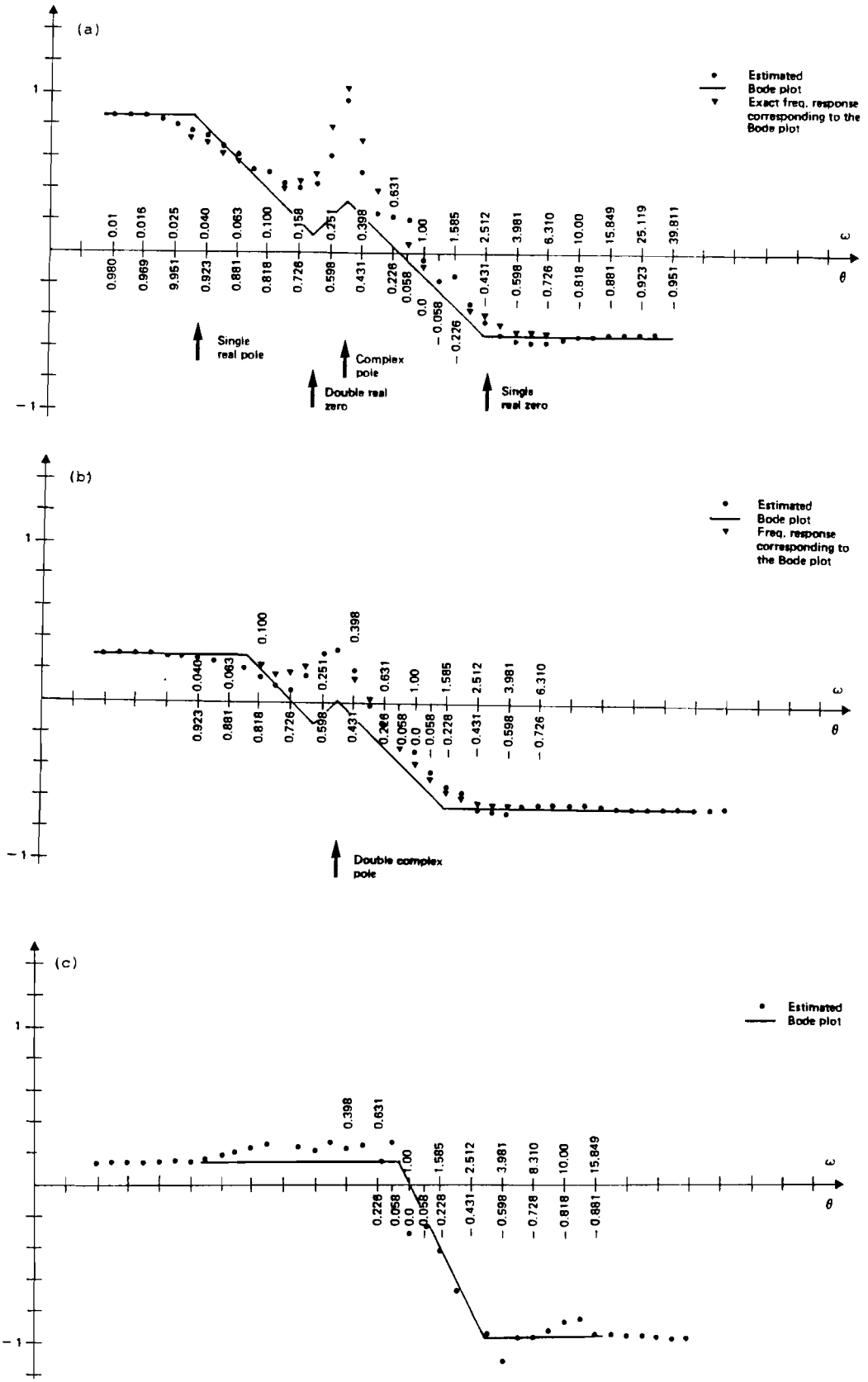

FIGURE 26 Bode plots for time series E from Box and Jenkins: (a) ARSPEC estimate; (b) BT estimate; (c) GSPEC estimate.

$$G(z) = \frac{(1-0.634z)^2(1+0.226z)}{(1-0.853z)(1-1.36z+0.665z^2)} \quad . \tag{89}$$

As usual, the GSPEC estimator gave rather bad results, no peak occurring on the frequency response plot. With differenced data we again obtained results which could not be interpreted in any reasonable way.

It is interesting to compare the models identified here with the Box–Jenkins solutions. The Box–Jenkins models have the following transfer functions:

$$G_1(z) = \frac{1}{1-1.42z+0.73z^2} \quad , \tag{90}$$

$$G_2(z) = \frac{1}{1-1.57z+1.02z^2-0.21z^3} \quad . \tag{91}$$

The Bode plots for the above models are presented in Figure 27(a,b). A number of other models of this series have also been investigated — Ozaki (1977) tested some high-order models, and two new models have been proposed by Woodward and Gray (1978). Again, it would be interesting to analyze these models using the technique presented here.

Both Box–Jenkins models give rather a bad fit. The amplitude of the peak is too small, and for low frequencies the frequency response does not correspond to the SDF at all. The Ozaki ARMA(3,6) model produces some interesting results (see Figure 28): it gives a perfect fit for high frequencies but for low frequencies its behavior is extremely bad —an unnecessary peak can be observed for $\omega \simeq 0.03$. This suggests that the model is overparametrized.

This additional peak is generated by a double complex pole at $\omega \simeq 0.04$; a single pole would actually give the Bode plot a reasonable shape at low frequencies. It can also be seen that the slope of the asymptote for $\omega \simeq 0.04-0.1$ is -3. This means that there is a single real root in this region. Removing this root

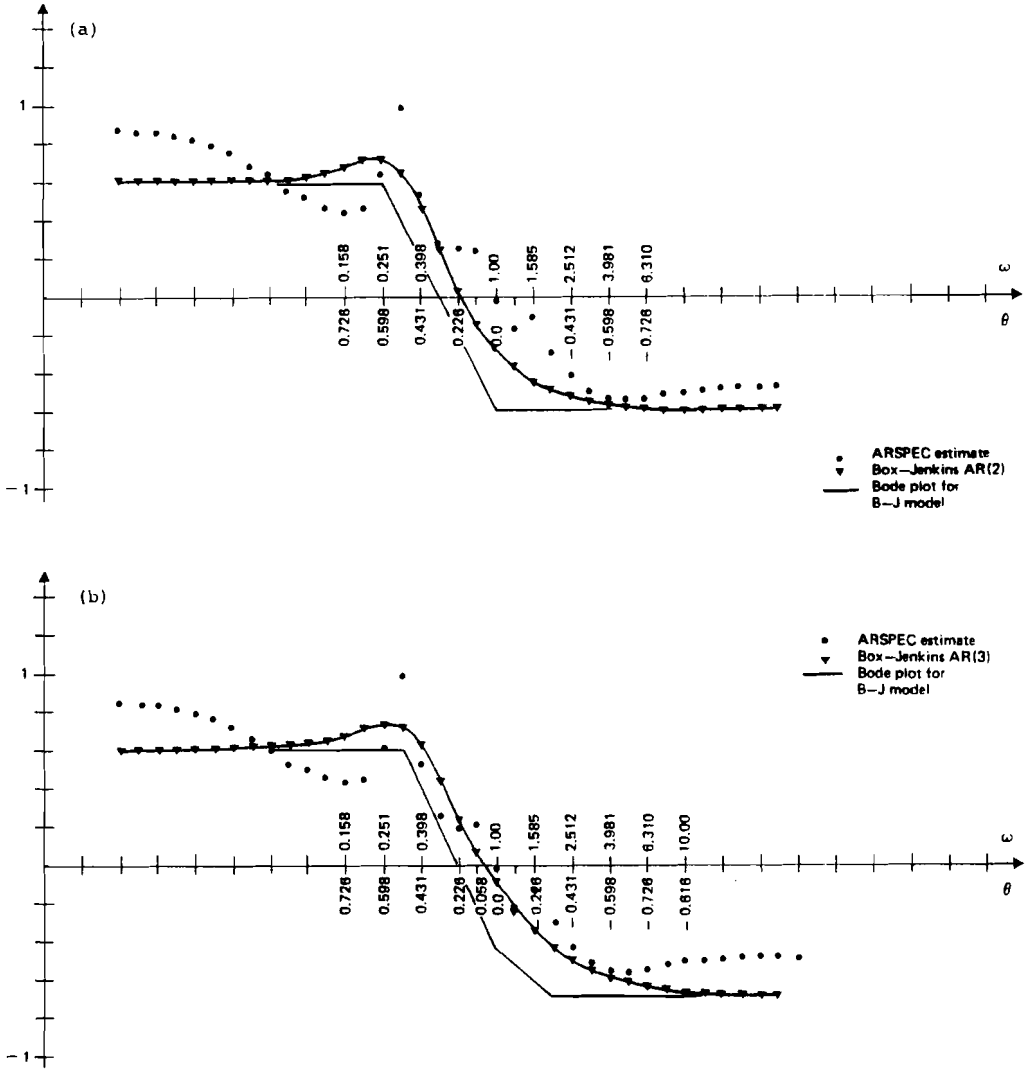

FIGURE 27 Bode plots for (a) Box and Jenkins' AR(2) model and (b) Box and Jenkins' AR(3) model of time series E (Wolfer's sunspot numbers), compared with the ARSPEC estimate of the spectral density function.

should give a frequency response of the required shape. The behavior of the two models proposed by Woodward and Gray is very good; the ARMA(2,6) model gives a better fit at low frequencies than the alternative ARMA(6,1) model (see Figure 29).

Example 13. Now we shall try to apply our methodology to seasonal time series. Consider series G from Box and Jenkins (1970). The linearized spectrum of this time series is presented in Figure 30(a). Theoretical investigations

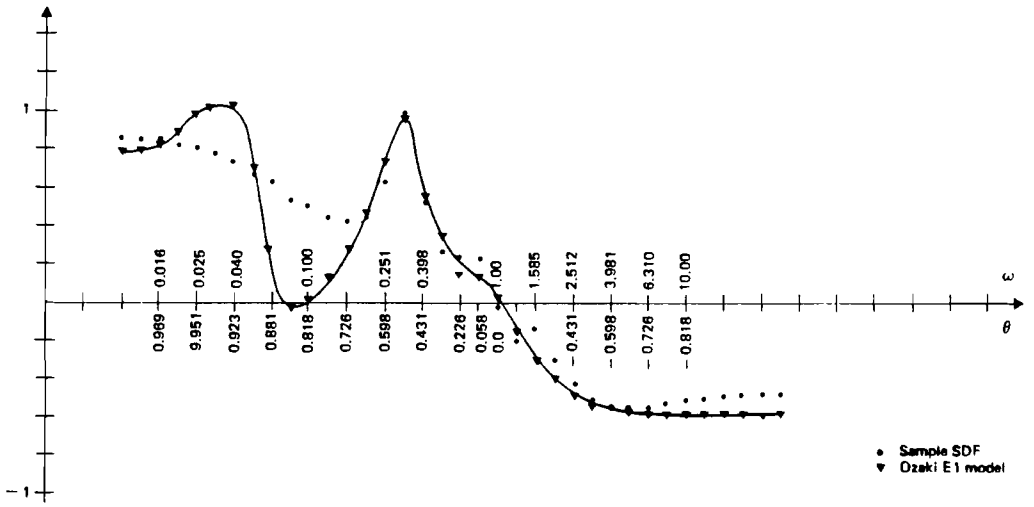

FIGURE 28 Bode plot for Ozaki's model of time series E (Wolfer's sunspot numbers) compared with the ARSPEC estimate of the spectral density function.

show that this plot should have 5 peaks (if the period of the time series is 12). These peaks are easily identified on the plot. Analyzing the height of these peaks, we conclude that the transfer function of the seasonal factor is

$$\frac{1}{1-0.975z^{12}} \,. \tag{92}$$

Thus the estimated frequency response function reproduces the theoretical response very well for $\omega \gg 1$. However, the differences observed at lower frequencies are quite significant — to analyze these in more depth this part of the plot is displayed in Figure 30(b). The suggested form of the transfer function is as follows:

$$G(z) = h(z)\frac{1}{1-0.975z^{12}} \tag{93}$$

where $h(z)$ should be chosen such that it

(i) does not destroy the good fit for high frequencies, i.e., $\log|h(j\omega)| \simeq 0$ for $\omega > 1$;

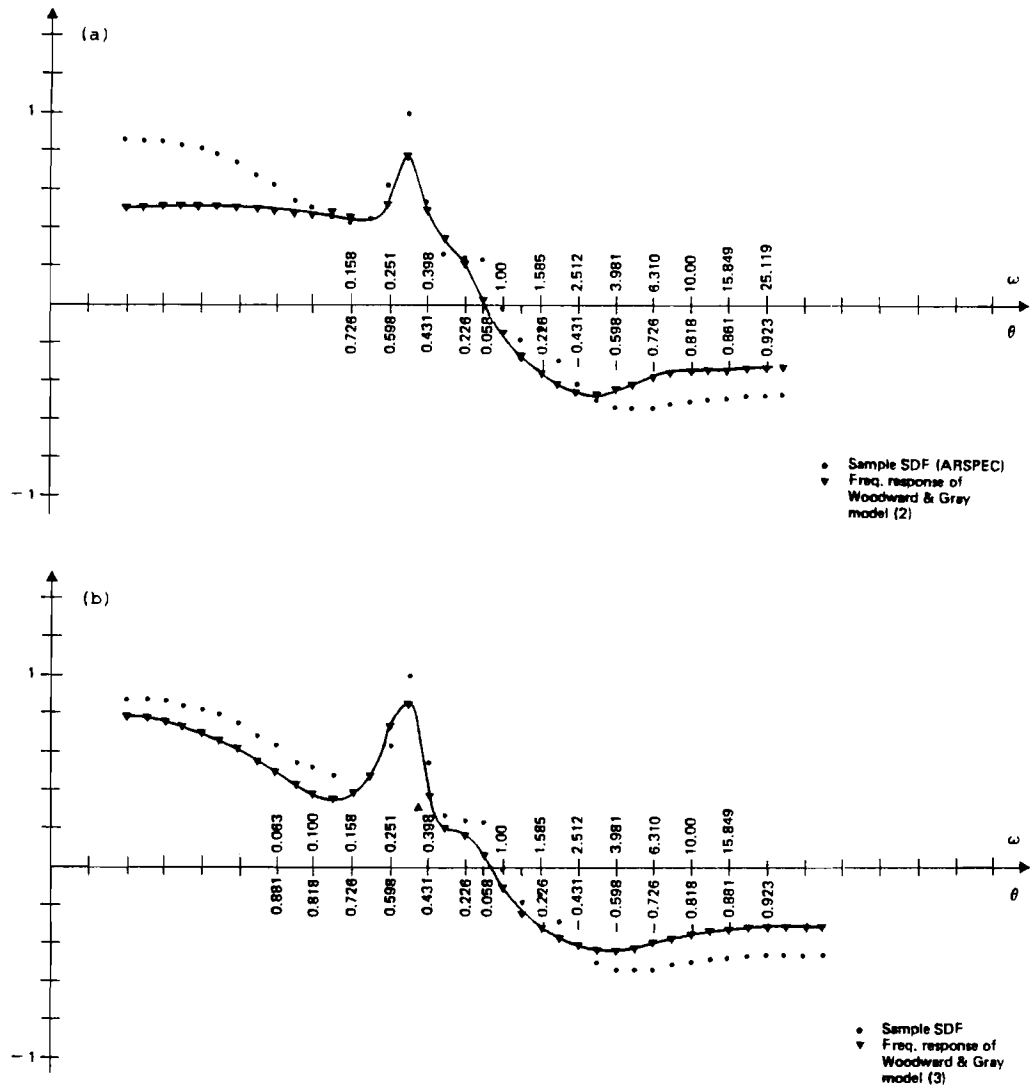

FIGURE 29 Bode plots for (a) Woodward and Gray's ARMA(6,1) model and (b) Woodward and Gray's ARMA (2,6) model of time series E (Wolfer's sunspot numbers) compared with the ARSPEC estimate of the spectral density function.

(ii) corrects the low-frequency part of the frequency response.

On analyzing Figure 30(b), we conclude that the most important thing is to cancel the pole at $\omega = 0.001$; for this reason the "correcting filter" must have a zero at this frequency. The rest of the $h(z)$ frequency response is determined by the first requirement, which means that the transfer function should have two poles and one zero. The suggested form of the Bode plot is presented in Figure 30(b) (solid line); the theoretical frequency response function is also

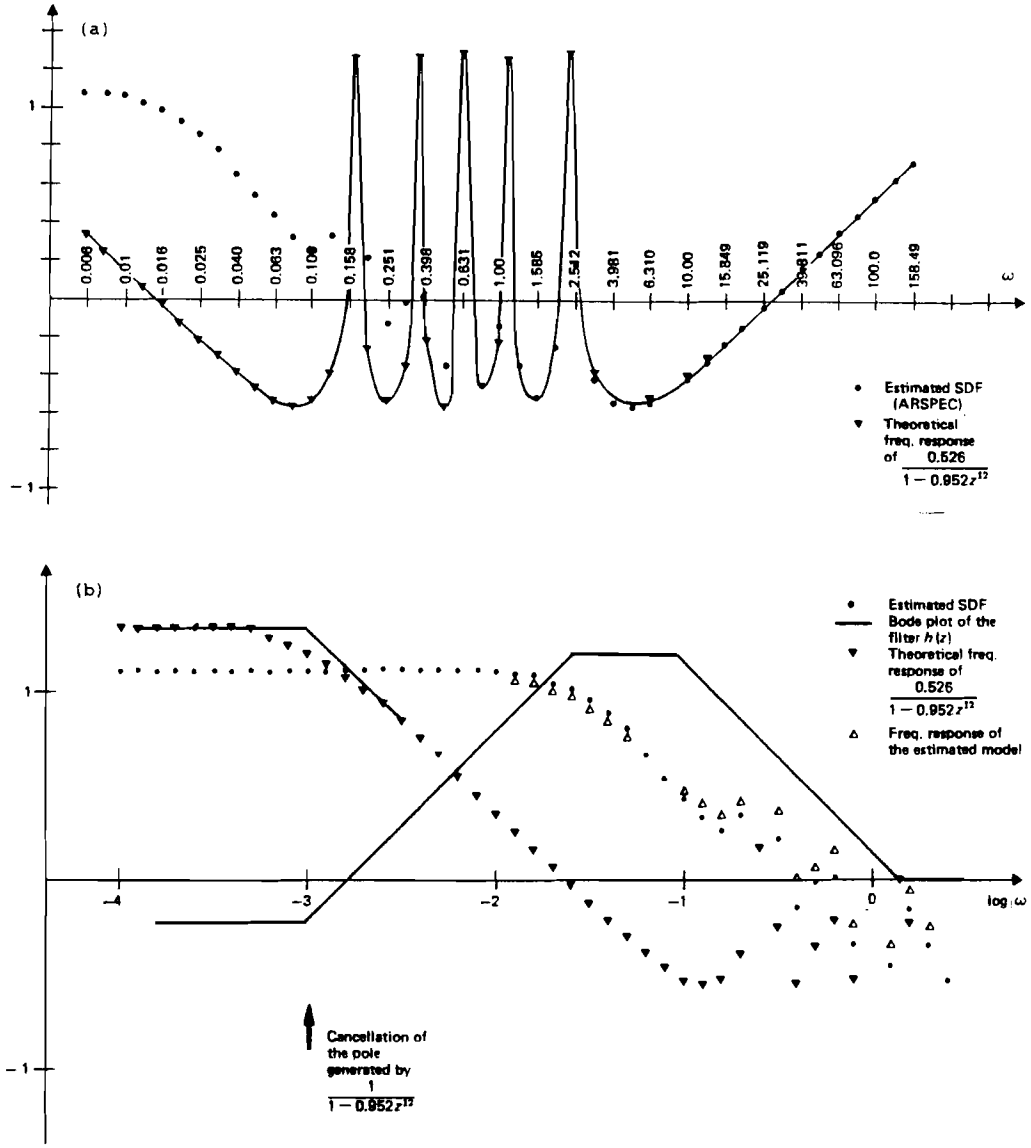

FIGURE 30 (a) Spectral density function for time series G from Box and Jenkins compared with the theoretical frequency response plot for seasonal model $\frac{0.526}{1-0.952z^{12}}$; (b) expansion of the low-frequency part of (a) together with the Bode plot of the "correcting" filter.

given. We see that the fit is very good. This leads to the following model:

$$G(z) = \frac{(1-0.988z)(1+0.171z)}{(1-0.951z)(1-0.833z)(1-0.952z^{12})} . \tag{94}$$

This procedure was repeated using differenced data; the results are displayed in Figure 31. In this case the situation is not so complicated and con-

sequently the structure of the correcting filter is very simple. The final model has the following form:

$$G(z) = \frac{(1-0.998z)}{(1-z)(1-0.939z)(1-0.975z^{12})} . \tag{95}$$

It would be interesting to compare this model with those obtained by Box and Jenkins; however, this cannot be done in the frequency domain because the seasonal differencing procedure proposed by Box and Jenkins causes infinite peaks in the frequency response. To check the accuracy of the identification procedure we estimated the parameters of a number of models differing in structure using the MINITAB system.

The results are collected in Table 5. It can be observed that model 4 corresponds very well to (95) and model 5 to (94). It should be noted that the estimation was carried out following identification using the method proposed in this paper.

4.3. Gas Consumption Data

Example 14. This time series was analyzed by the author during research on the control of a natural gas transmission system. One of the basic problems was to develop an algorithm predicting gas consumption. The time series analyzed in this section is the consumption of gas at the same hour each day, over a one-year period. The frequency responses of this time series (rough and differenced) are presented in Figure 32(a,b). The situation is in general similar to that described in Example 13, except that the amplitude of the peaks is smaller. The amplitude of the last peak can be used to determine the value of the parameter ϑ in the seasonal AR term — after simple analysis a value of 0.25 was obtained. Next, we use our standard approach to plot the theoretical frequency response of the seasonal factor. This is illustrated in Figure 33. The situation is again similar to that described in Example 13 — the fit is good for

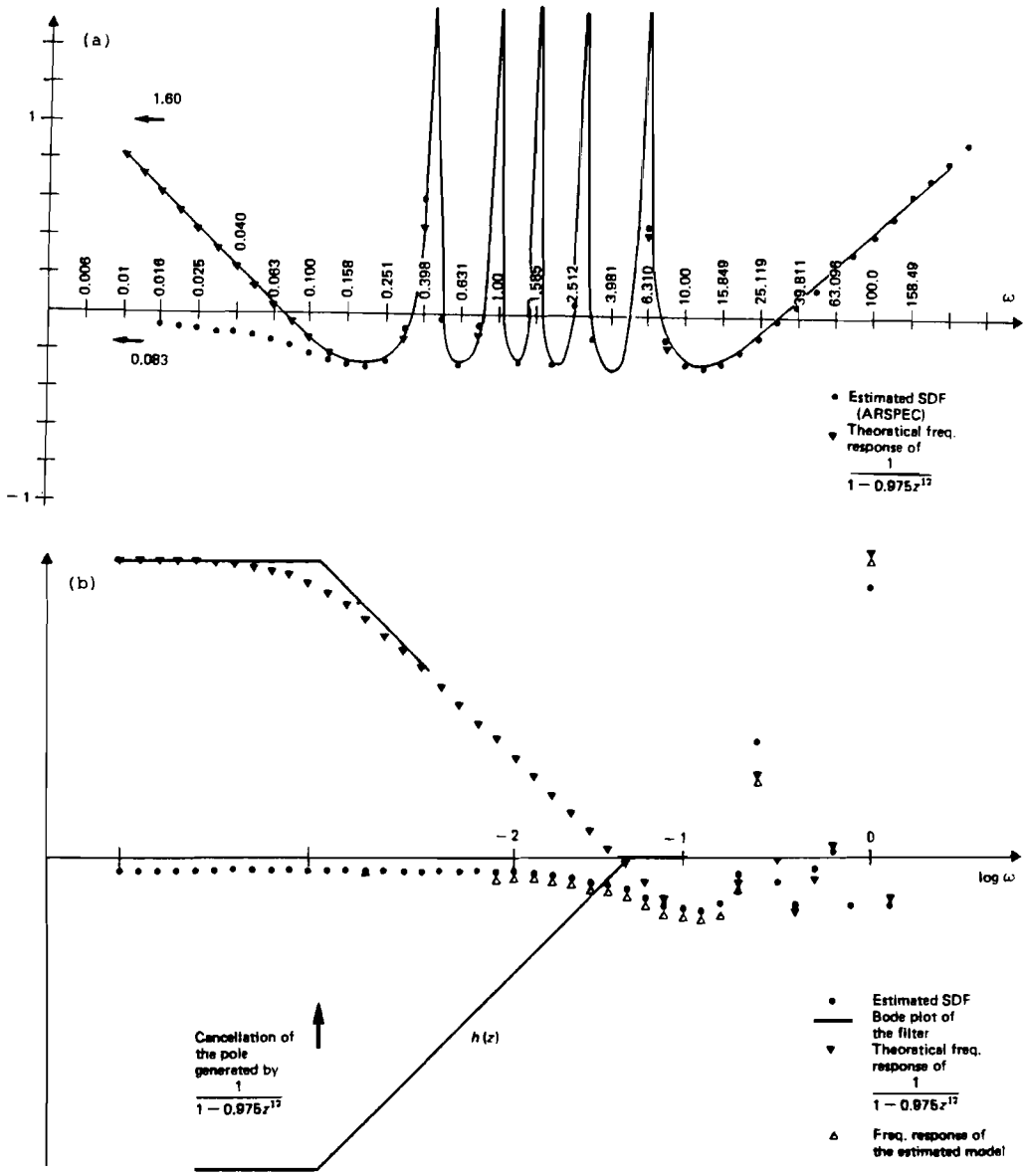

FIGURE 31 (a) Spectral density function for ***differenced*** time series G from Box and Jenkins compared with the theoretical frequency response plot for seasonal model $\frac{1}{1-0.975z^{12}}$; (b) expansion of the low-frequency part of (a) together with the Bode plot of the "correcting" filter.

high frequencies. We now have to design a low-frequency filter which will modify the low-frequency part of the characteristics. To do this we carry out "deseasonal filtering" . This is a very simple graphical procedure in which it is only necessary to subtract from the estimated response function the following theoretical response function:

TABLE 5. Identification of time series G from Box and Jenkins (1970) using the MINITAB package.

Model no.	Model description	Sum of squared errors
1	$\frac{(1+0.098z^{12})(1-0.18z)}{(1-z)(1-z^{12})}$	367
2	$\frac{(1+0.09z^{12})(1-0.878z)}{(1-z)(1-z^{12})(1-0.0711z)}$	361
3	$\frac{(1-0.876z)}{(1-z)(1-z^{12})(1-0.096z^{12})(1-0.71z)}$	361
4	$\frac{(1-0.993z)}{(1-z)(1-0.845z)(1-0.99z^{12})}$	328
5	$\frac{(1-0.775z)(1-0.07z)}{(1-0.725z)(1-0.906z)(1-0.993z^{12})}$	326

$$G(z) = \frac{1}{1-0.25z^{7}} \tag{96}$$

which corresponds to the seasonal factor transfer function. The result is presented in Figure 33; the next step is to fit the non-seasonal model. A peak can now be observed at $\omega \simeq 0.2$; the question is whether this peak is caused by the pair of complex roots or not. These two possibilities are analyzed in Figures 34 and 35. It can be seen that the model with complex roots gives a better fit; however, its transfer function is rather complicated:

$$G(z) = \frac{(1-0.826z)(1-0.667z)^2}{(1+5.01z+25.1z^2)(1-0.25z^7)(1-z)} \tag{97}$$

The other hypothesis leads to the following result:

$$G(z) = \frac{(1-0.903z)(1-.230z)}{(1-0.583z)(1-0.246z^7)(1-z)} \tag{98}$$

The same procedure could be followed using the rough (non-differenced) data; the major difference is that instead of the AR factor $(1-z)$ we obtain $1-0.998z$, which suggests the need to differentiate the time series.

It is interesting to note that a simpler model can be proposed, i.e., one in which the non-seasonal component has AR(1,1) structure:

$$G(z) = \frac{(1-0.85z)}{(1-0.23z)(1-z)} . \tag{99}$$

The frequency response of this model is presented in Figure 36.

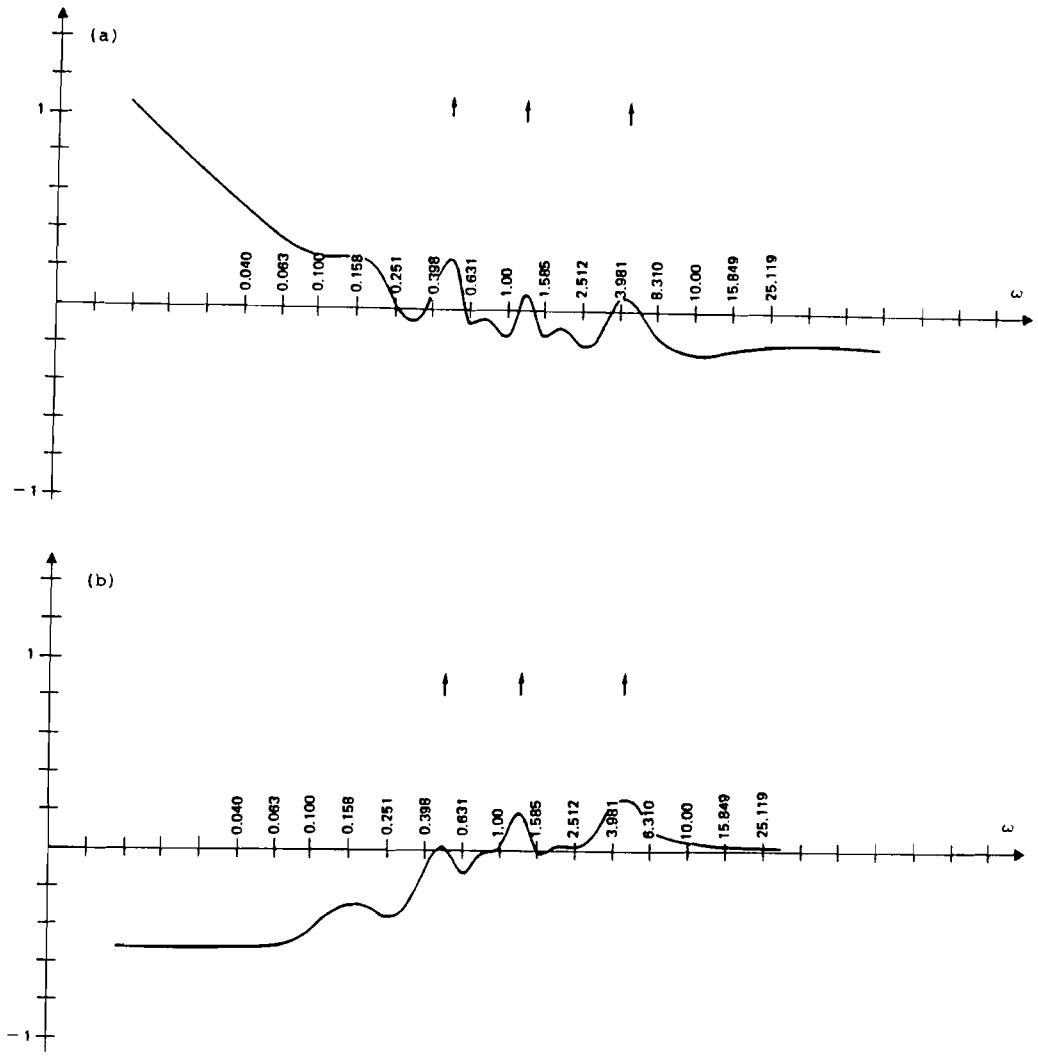

FIGURE 32 Spectral density functions of some (a) rough and (b) differenced gas consumption data, ARSPEC estimates.

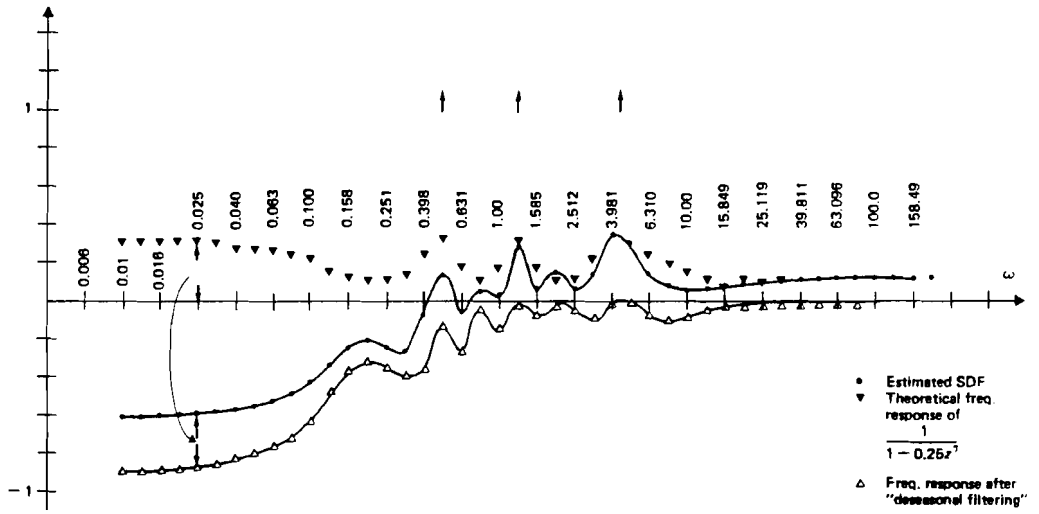

FIGURE 33 The "deseasonal filtering" of some differenced gas consumption data.

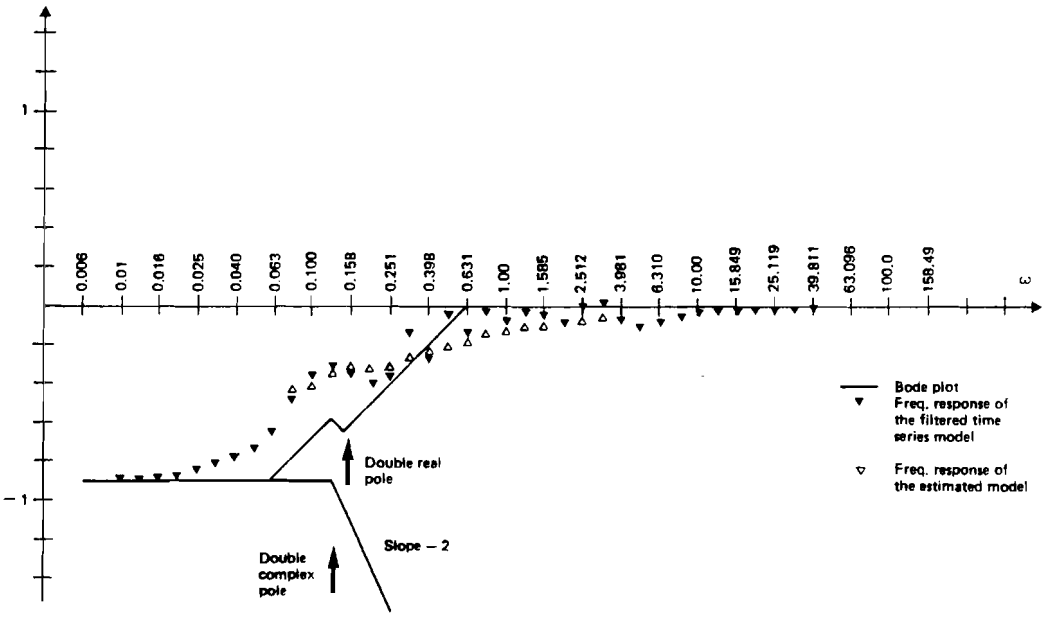

FIGURE 34 Bode plot of the non-seasonal part of the gas consumption data considered above. Complex pole assumed at $\omega \simeq 0.2$.

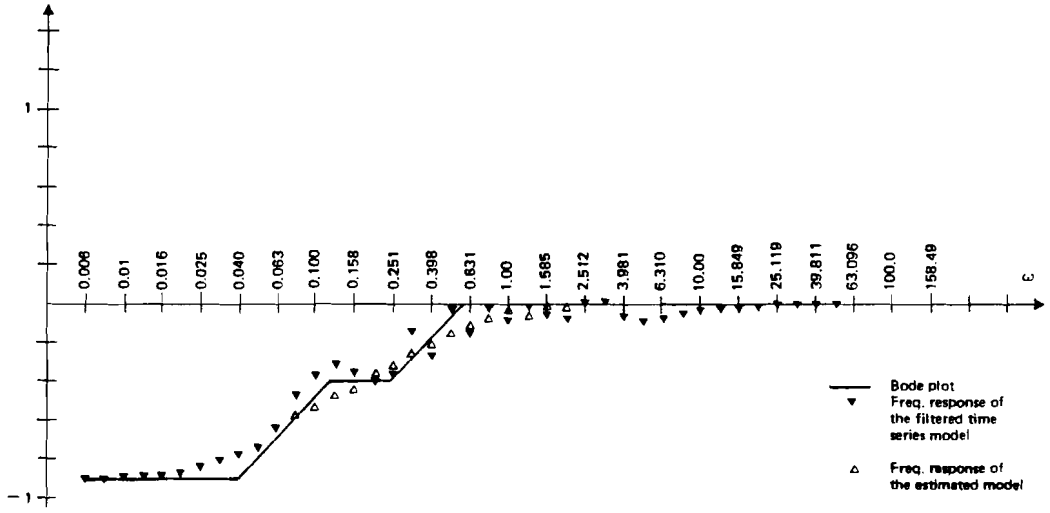

FIGURE 35 Bode plot of the non-seasonal part of the gas consumption data considered above. No complex poles are assumed.

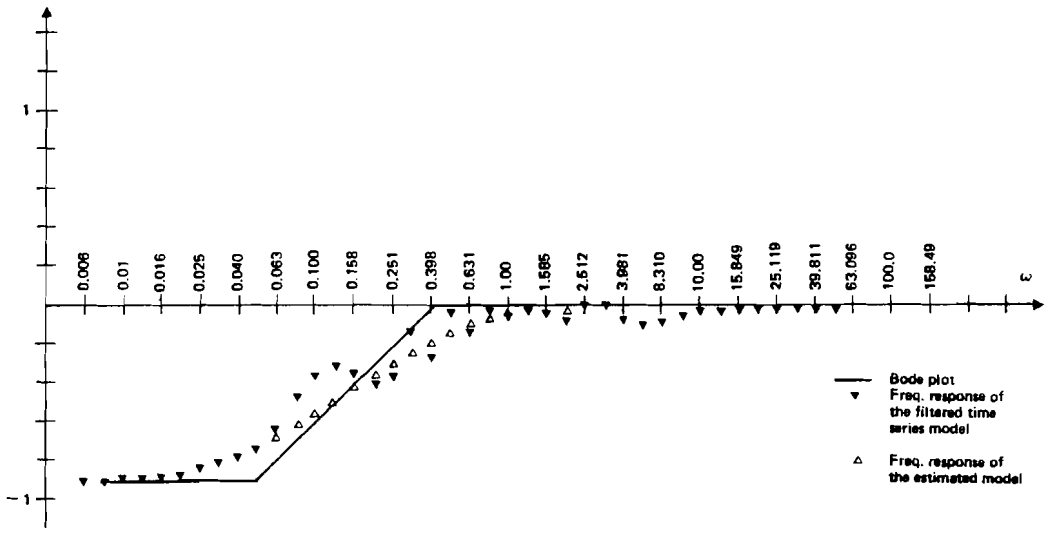

FIGURE 36 Bode plot of the non-seasonal part of the gas consumption data — the simplest model with AR(1,1) nonseasonal factor.

5. CONCLUSIONS

It should be emphasized that the method presented in this paper is not proposed as a universal solution of the identification problem. The author does not agree with Anderson (1980) that

> "it is understandable for innovators to be enthusiastic whilst others are conservatively (perhaps, enviously) less optimistic".

The author does not overestimate the role of the method — he believes that it simply bridges the gap between the rich collection of methods for *estimating spectra* and methods for *analyzing and understanding* them. Moreover, this method cannot be used in isolation. Parzen (1980) tells us that:

> "...it seems critical that a successful approach to time series modeling employ simultaneously both the spectral domain and the time domain."

The importance of this statement can be deduced from the examples presented in this paper. There are many situations in which analysis of the ACF gives more information than analysis of the frequency response function. This is mainly the case for pure MA processes, where the structure of the ACF is often very clear and the properties of the spectral estimates relatively bad. However, on the other hand there are also many cases in which it can be difficult to interpret the ACF, and analysis of the spectral density function can be of considerable use.

REFERENCES

Akaike, H. (1974). A new look at the statistical model identification. *IEEE Trans. on Automatic Control*, Vol. AC19.

Anderson, O.D. (1980). A new approach to ARMA modeling: some comments. In O.D. Anderson (Ed.), *Analyzing Time Series*, North-Holland Publ. Co., Amsterdam.

Anderson, T.E. (1971). *The Statistical Analysis of Time Series*. John Wiley and Sons.

Beamish, N. and M.B. Priestley (1981). A study of autoregressive and window spectral estimation. *Appl. Stat.*, Vol. 30, No. 1.

Beguin, J.M., Ch. Gourieroux and A. Monfort (1980). Identification of a mixed autoregressive moving average process: the corner method. In O.D. Anderson (Ed.), *Time Series*, North-Holland Publ. Co., Amsterdam.

Bishop, A.B. (1975). *Introduction to Discrete Linear Controls, Theory and Application*. Academic Press.

Box, G.E.P. and G.M. Jenkins (1970). *Time Series Analysis, Forecasting and Control*. Holden-Day.

Cadzow, J.A. (1973). *Discrete Time Systems*. Prentice-Hall.

D'Azzo, J.J. and C.H. Houpis (1975). *Linear Control Systems: Analysis and Design*. McGraw-Hill.

De Gooijer, J.G. and R.M.J. Hents (1981). The corner method: an investigation of an order discrimination procedure for general ARMA processes. University of Amsterdam, Faculty of Agricultural Science and Econometrics, Report AE 9/81.

Digital Signal Processing Committee (Ed.) (1979). Programs for Digital Signal Processing. IEEE Acoustics, Speech and Signal Processing Society, IEEE

Press, 1979.

Gray, H.L., G.D. Kelley and D.D. McIntire (1978). A new approach to ARMA modeling. *Comm. Stat., Ser. B*, Vol. 7.

Gray, H.L., A.G. Houston and F.W. Morgan (1978). On G-spectral estimation. In D.F. Findley (Ed.), *Applied Time Series Analysis*, Academic Press.

Hannan, E.J. (1960). *Time Series Analysis*. Methuen.

Hannan, E.J. (1970). *Multiple Time Series*. John Wiley and Sons.

Jenkins, G.M. and D.G. Watts (1968). *Spectral Analysis and its Application*. Holden-Day.

Jones, R.H. (1978). Multivariate autoregression estimation using residuals. In D.F. Findley (Ed.), *Applied Time Series Analysis*, Academic Press.

de Jong, P. (1977). The fast fourier transform spectral estimator. *J. Roy. Stat. Soc., Ser. B*, Vol. 39, No. 3.

Kalman, R.E., P.L. Falb and M.A. Arbib (1969). *Topics in Mathematical System Theory*. McGraw-Hill.

Kleiner, B., R.D. Martin and D.J. Thomson (1979). Robust estimation of power spectra. *J. Roy. Stat. Soc., Ser. B*, Vol. 41, No.3.

Koopmans, L.H. (1974). *The Spectral Analysis of Time Series*. Academic Press.

Lago, G. and L.M. Benningfield (1979). *Circuit and System Theory*. John Wiley and Sons.

Makridakis, S. (1976). A survey of time series. *Int. Stat. Rev.*, Vol. 44.

Martin, R.D. (1979). Robust estimation for time series autoregression. In R.L. Launer and G.N. Wilkinson (Eds.), *Robustness in Statistics*, Academic Press.

Martin, R.D. (1980). Robust estimation of autoregressive models. In D.R. Brillinger and G.C. Tiao (Eds.), *Reports on Directions in Time Series*, Institute of Mathematical Statistics.

Nerlowe, M., D.M. Grander and J.L. Carvalho (1979). *Analysis of Economic Time Series: A Synthesis*. Academic Press.

Otnes, R.K. and L. Enochson (1978). *Applied Time Series Analysis*. John Wiley and Sons.

Ozaki, T. (1977). On the order determination of ARIMA models. *Appl. Stat.*, Vol. 26, No. 3.

Parzen, E. (1980). Time series modeling, spectral analysis and forecasting. In D.R. Brillinger and G.C. Tiao (Eds.), *Reports on Directions in Time Series*, Institute of Mathematical Statistics.

Polasek, W. (1979). Identification of SARIMA processes: a classification of seasonal models. Institute of Statistics, Vienna University, Report No. 10.

Polasek, W. (1980). ACF patterns in seasonal MA processes. In O.D. Anderson (Ed.), *Time Series*, North-Holland Publ. Co., Amsterdam.

Priestley, M.B. (1981). *Spectral Analysis of Time Series*. Academic Press.

Robinson, E.A. (1981). Realizability and minimum delay aspects of multichannel models. In E.A. Robinson (Ed.), *Time Series Analysis and Applications*, Goose Pond Press.

Sage, A.P. (1981). *Linear System Control*. Pitman Press.

Silverman, H. (1975). *Complex Variables*. Houghton-Mifflin.

Ulrych, T.L. (1975). Maximum entropy spectral analysis and autoregressive decomposition. *Rev. Geophysics Space Physics*, Vol. 13, No. 1.

Woodward, W.A. and H.L. Gray (1978). New ARMA models for Wolfer's sunspot data. *Comm. Stat.*, Vol. B7, No. 1.

APPENDIX A: METHODS FOR ESTIMATING SPECTRAL DENSITY FUNCTIONS

It is obvious that the use of the methods described in this paper is dependent on having sufficiently efficient algorithms for spectrum estimation. Fortunately, there are currently at least three groups of such algorithms. A review of existing techniques has recently been carried out by Priestley (1981). We shall provide here only a brief outline of the various methods of spectrum estimation.

ACF Fourier Transformation

This is the best-known method for estimating a spectral density function. In this formulation the spectrum is computed using the following equation:

$$f(\omega) = \frac{1}{2\pi} \sum_{p=-\infty}^{+\infty} e^{-j\omega p} c_p \qquad (A.1)$$

where c_p is the value of the ACF for lag p. This formula can be used directly for density function estimation; the only difficulty is caused by the fact that we can estimate the ACF only for a finite number of lags. This causes certain distortions in the spectrum; to avoid this it is necessary to use a *window* q_p. The corresponding formula for estimating the spectral density is as follows:

$$f(\omega) = \frac{1}{2\pi} \sum_{p=-N}^{+N} e^{-j\omega p} c_p q_p \qquad (A.2)$$

One of the possible windows is the *Bartlett window* :

$$q_p = \begin{cases} 1 - \frac{|p|}{N} & \text{for } \frac{|p|}{N} < 1 \\ 0 & \text{otherwise} \end{cases} \qquad (A.3)$$

Many other types of windows have been proposed. The statistical properties of (A.2) have been analyzed in a number of publications, the best-known of which is the classic textbook by Jenkins and Watts (1968); others include Koopmans (1974), Hannan (1960), Anderson (1971) and Priestley (1981).

It should be noted that the parameter N in (A.2) determines the properties of the spectral estimator (the so-called *resolution* or *bandwidth*) and also the standard error of the estimate. In general, large N ensures high resolution, so that we can detect the narrow peaks in the spectrum. On the other hand, a high value of N also causes a large variance in the estimator. Small N ensures a small variance but increases the bias and causes more distortion of the spectrum, since the "spectral window" is wider. For these reasons it is necessary to find a compromise value of N. The usual procedure is to calculate density functions for different values of N and then compare the results.

G-Transform Estimator (GSPEC Estimator)

This method is an extension of the previous one. The basic principle is to use the algorithm for accelerated summation of infinite series to calculate (A.1). This special class of algorithms was introduced and investigated by Gray, Houston and Morgan (1978). Under the assumption that the time series has ARMA structure, they showed that the proposed estimator converges; however, nothing is known about its statistical properties. The corresponding computer program has also been published (Gray et al., 1978). The developers of this method are enthusiastic about it; however, the experience of the present author is that the method does not always work. It appears that the GSPEC estimator works properly only for time series which are low-order ARMA; it does not work at all for pure MA or seasonal time series. For these reasons this approach cannot be recommended.

Direct Data Transformation

A number of new techniques based on Fast Fourier Transform (FFT) have been developed. These involve direct Fourier transformation of the data. In order to avoid distortion of the spectrum an operation similar to windowing must be performed, but in the time domain. Because of the high efficiency of FFT, these methods are especially suitable for long time series. An excellent review of FFT methods and related algorithms is given by Otnes and Enochson (1978) and various associated computer programs have been prepared by the Digital Signal Processing Committee under the title "Programs for Digital Signal Processing" (1979). From a statistical point of view, these methods are equivalent to ACF-based estimators (see, for example, de Jong, 1977).

Autoregressive Estimator (ARSPEC)

This is a new class of very efficient spectral estimators which are almost as easy to compute as ACF-based estimators but in general have better properties. The basic idea of this method is simple —find the autoregressive model of the process under study

$$y_t = \sum_{p=1}^{N} a_p y_{t-p} \tag{A.4}$$

and using this model calculate the spectrum

$$f(\omega) = \frac{\sigma^2}{|1 - \sum_{p=1}^{N} a_p e^{-jp\omega}|^2} \quad . \tag{A.5}$$

The basic assumption is that the investigated process has high-order or infinite-order AR representation. The conditions under which this representation exists have been investigated, e.g., by Koopmans (1974). However, it is not very difficult to construct a time series for which such a representation does not exist, e.g.,

$$y_t = \varepsilon_t + 2\varepsilon_{t-1} \quad . \tag{A.6}$$

The possible nonexistence of an AR representation is potentially one of the most important problems with this method, although in the author's experience such situations rarely occur in the analysis of real time series data.

In order to use this technique it is necessary to:

—choose the appropriate technique for AR model estimation;

—determine the order of the AR model.

There are several ways of doing this, most of which have been discussed in detail by Ulrych (1975); his paper also contains two efficient Fortran subroutines. In general there are two methods of estimation —one is based on a sample autocorrelation function and the Yule–Walker equations, while the other involves direct estimation from the data using a modified prediction-error algorithm. The best known method of order determination is the Akaike criterion (Akaike, 1974). According to this criterion, the best model is that which minimizes the function

$$n \log |S_p| + 2N \tag{A.7}$$

where n is the length of the time series, S_p is an estimate of σ^2 (one-step-ahead prediction variance), and N is the order of the AR model.

This procedure has been examined empirically by Ozaki (1977). The theory and properties of the Akaike procedure have also been investigated by many other authors; a selected bibliography can be found in Appendix C. A method based on the prediction error approach was adopted in this paper; the computer program was taken from Jones (1978).

Related Topics

Another important aspect of spectrum estimation concerns the *sensitivity* of the estimator. There are two possible sources of error: missing data and measurement errors ("outliers"). Empirical investigation shows that even small deviations can cause significant distortion of the estimated spectrum, especially at high frequencies. This problem has recently been analyzed in great detail; the basic results are presented in Kleiner et al., (1979) and Martin (1979, 1980) . Of especial interest is the recent paper by Martin (1980), which presents robust methods for AR model estimation, together with an Akaike-type approach for order determination. However, the author has no experience with these methods as yet.

APPENDIX B: ALTERNATIVE APPROACHES IN TIME SERIES IDENTIFICATION

There are a number of alternative approaches for time series identification. That proposed by Box and Jenkins (1970) based on the "visual inspection" of the ACF is undoubtedly the simplest. However, in practice it is often difficult to interpret the sample ACF (or even the theoretical ACF); still, the experienced analyst can usually extract some useful information from the ACF. It has been suggested that a "catalogue" of possible ACFs should be created or that the set of possible models should be structured in some way. An ACF catalogue would be a kind of handbook for the analyst. This idea was explored by Polasek, who has investigated and classified the possible structures of seasonal MA models (Polasek, 1980). Using this taxonomy, a catalogue of possible ACF patterns has been prepared (Polasek, 1979). The only thing the analyst has to do is to compute the ACF and then search through the catalogue to find the most similar ACF pattern. This method has two main disadvantages — the number of possible patterns may be large (over 100 in Polasek's catalogue) and determining the degree of similarity can be difficult. It should be quite possible to automate the procedure using a pattern recognition approach — however, this has not yet been done.

The other approaches utilize the known fact that if a time series has ARMA(p,q) structure, then the theoretical ACF for lags greater than q satisfies a linear difference equation of order p (e.g., Anderson, 1971). Thus, the idea is to check whether a subsequence of the ACF satisfies a linear difference equa-

tion. This can be done by several methods, all of which have a very strong connection with Kalman realization theory (Kalman et al., 1969). This theory is based on testing the rank of a matrix derived from the ACF (Henkel matrix). An algorithm for testing this rank has been proposed by Beguin et al. (1980). Another indicator of the rank of a Henkel matrix has been introduced by Gray, Kelley and McIntire (1978); this approach has been discussed by Anderson (1980). The basic difficulty in applying these methods (and which can even prevent them from being used) is connected with the fact that the computation of rank is an ill-defined problem. The source of this trouble is the binary character of rank testing — a matrix either has rank K or it does not. Thus, it takes only a small distortion of one matrix element to change its rank. There is a well-known statement that "every matrix in a computer is of full rank". The experiments performed by the author with realization algorithms have shown that they are almost useless for sample ACFs and must be applied and interpreted with the greatest care. The main disadvantage of these methods, however, is caused by the fact that instead of "visual inspection" of the ACF the analyst must use the same visual inspection procedure to analyze the columns of two matrices. The author's experience has shown that this can be extremely difficult. A recent analysis of this approach by De Goojier and Hents (1981) has shown that this method has limited applicability.

APPENDIX C: SELECTED BIBLIOGRAPHY ON SPECTRAL ANALYSIS AND ITS APPLICATIONS IN TIME SERIES IDENTIFICATION

Maximum Entropy Spectral Estimators

H. Akaike. Power spectrum estimation through autoregressive model fitting. *Ann. Inst. Stat. Math.*, Vol. 21, 1968.

J. Capon. High resolution frequency wavenumber spectrum analysis. *Proceedings of the IEEE*, Vol. 57, No. 8, August 1968.

J.P. Burg. The relationship between maximum entropy spectra and maximum likelihood spectra. *Geophysics*, Vol. 37, No. 2, April 1972.

W. Gersh and D.R. Sharpe. Estimation of power spectra with finite order autoregressive models. *IEEE Trans. on Automatic Control*, August 1973.

R.H. Jones. Identification and autoregressive spectrum estimation. *IEEE Trans. on Automatic Control*, Vol. AC19, December 1974.

E. Parzen. Some recent advances in time series modelling. *IEEE Trans. on Automatic Control*, Vol. AC19, December 1974.

K.N. Bek. Consistent autoregressive spectral estimates. *Annals of Statistics*, Vol. 2, 1974.

T.L. Ulrych. Maximum entropy spectral analysis and autoregressive decomposition. *Rev. Geophysics and Space Physics*, Vol. 13, No. 1, 1975.

M. Kareh and G.R. Cooper. An empirical investigation of the properties of the autoregressive spectral estimator. *IEEE Trans. on Information Theory*, Vol. IT22, No. 3, 1976.

A.B. Baggeroer. Confidence intervals for regression (MEM) spectral estimates.

IEEE Trans. on Information Theory, Vol. IT22, No. 5, 1976.

W.I. Newman. Extension to the maximum entropy method I. *IEEE Trans. on Information Theory*, Vol. IT23, No. 1, 1977.

D. McIntire. A comparative study of several spectral estimates. In D.F.Findley (Ed.), *Applied Time Series Analysis*, Academic Press, 1978.

W.I. Newman. Extension to the maximum entropy method II. *IEEE Trans. on Information Theory*, IT25, No. 6, 1979.

N. Beamish and M.B. Priestley. A study of autoregressive and window spectral estimation. *Appl. Stat.*, Vol. 30, No. 1, 1981.

Spectral Methods in Time Series Identification and Model Estimation

L.H. Koopmans. *The Spectral Analysis of Time Series*, Academic Press, 1974.

T.W. Anderson. Estimation for autoregressive moving average models in the time and frequency domains. *Annals of Statistics*, Vol. 5, 1977.

L. Ljung and K. Gloveer. Frequency domain versus time domain methods in system identification: a brief discussion. In *Proceedings of the Fifth IFAC Symposium on Identification and Parameter Estimation*, Darmstadt, FRG, 24–28 September 1979. Published for IFAC by Academic Press.

M. Nerlowe, D.M. Grander and J.L. Carvalho. *Analysis of Economic Time Series: A Synthesis*, Academic Press, 1979.

M.B. Priestley. *Spectral Analysis and Time Series*, Academic Press, 1981.

Methods for Time Series Identification

K.W. Hipel, A.I. McLeod and W.C. Lennox. Advances in Box–Jenkins modelling: 1. Model construction; 2. Applications. *Water Resources Research*, Vol. 13, No. 3, 1977.

H.L. Gray, G.D. Kelley and D.D. McIntire. A new approach to ARMA modelling.

Comm. Stat., Ser. B, Vol. 7, 1978.

C. Chatfield. Inverse autocorrelations. *J. Roy. Stat. Soc., Ser. A*, Vol. 142, 1979.

W. Polasek. Identification of SARIMA processes: a classification of seasonal models. Institute of Statistics, Vienna University, Report No. 10, 1979.

O.D. Anderson. A new approach to ARMA modelling: some comments. In O.D. Anderson (Ed.), *Analyzing Time Series*, North-Holland Publ. Co., 1980.

W.Polasek. ACF patterns in seasonal MA processes. In O.D. Anderson (Ed.), *Time Series*, North-Holland Publ. Co., 1980.

J.M. Beguin, Ch. Gourieroux and A. Monfort. Identification of mixed auto-regressive moving average processes: the corner method. In O.D. Anderson (Ed.), *Time Series*, North-Holland Publ. Co., 1980.

J.G. De Gooijer and R.M.J. Hents. The corner method: an investigation of an order discrimination procedure for general ARMA processes. University of Amsterdam, Faculty of Agricultural Science and Econometrics, Report AE 9/81.